REVISION STATUS SHEET

Document Title: Control Building Stability Analysis Report

Revision #: 0 **Type:** Engineering Report – Design

Safety Related Classification Code: N/A **MPL No.:** U73-5020

"|" Vertical Sidebar Denotes Change

Rev #	DOORS BL	Change Number	MM/DD/YYYY	Preparing Organization	Issue / Release Status	Verification Status
0	N/A	ECO-0015271	07/01/2015	GEH	Issued for Use-Design	Verified

MADE BY	APPROVALS	AUTH. DATE
Luben Todorovski GEH	Tanya B. Kirby GEH	07/01/2015

REVISION CHART (CONT)

Rev #	DOORS BL	Change Number	MM/DD/YYYY	Preparing Organization	Issue / Release Status	Verification Status

RECORD OF REVISION

Rev #	Description
0	Initial issue

TABLE OF CONTENTS

LIST OF TABLES

LIST OF FIGURES

LIST OF ACRONYMS

BE	Best Estimate
CB	Control Building
DCD	Design Control Document
EB	Energy Balance
EW	East-West
FS	Factor of Safety
LB	Lower Bound
MEB	Modified Energy Balance
NA3	North Anna Unit 3
NS	North-South
RB/FB	Reactor/Fuel Building Complex
SRP	Standard Review Plan
SSI	Soil-Structure Interaction
SSSI	Structure-Soil-Structure Interaction
UB	Upper Bound

1. INTRODUCTION AND PURPOSE

This report presents the North Anna Unit 3 (NA3) site-specific evaluations of the foundation seismic stability, dynamic bearing pressures and lateral pressures on the embedded exterior walls for the ESBWR Control Building (CB) that are based on the results of the site-specific soil-structure interaction (SSI) analyses presented in Reference 2-i. These evaluations use input parameters that are specific to the NA3 site and are based on seismic responses obtained from dynamic models representing full (uncracked concrete) stiffness properties of the CB reinforced concrete structure that, for the NA3 rock site with high frequency design motion, are conservative.

The stability of the CB is evaluated against overturning and sliding. The methodology used for the stability calculations is consistent with the methodology used for the standard design stability evaluations presented in the ESBWR Design Control Document (DCD) Tier 2 Subsection 3.8.5.5 (Reference 2-d).

The CB sliding stability evaluations consider two critical sliding planes located at :

- the bottom of the CB basemat located at El. 241 ft, NAVD88 (standard design El. -10.4 m), and
- the bottom of the underlying concrete fill located at nominal El. 225 ft, NAVD88 (standard design El. -15.31 m).

These sliding stability calculations provide the site-specific lateral pressure demands on the subgrade surrounding the CB at the NA3 site. The site-specific lateral pressure demands are compared with the lateral pressure capacity of the Zone III rock to demonstrate that the capacity of the subgrade is sufficient to ensure the sliding stability of the CB at the NA3 site.

The calculations of the maximum dynamic bearing pressure demands from the CB foundation to the supporting concrete fill follow the same Energy Balance (EB)/Modified Energy Balance (MEB) method that was used for the standard design calculations in Reference 2-f. These dynamic bearing pressure demands are compared with the allowable dynamic bearing pressure of the underlying concrete fill and Zone III-IV rock to ensure that the capacity of the subgrade is sufficient to resist the dynamic bearing pressures from the CB foundation.

The site-specific lateral pressure demands on the embedded exterior walls, presented in Section 7, are developed following the same methodology that is used for the standard design calculations in Reference 2-f and Reference 2-o.

1.1 Limitations on Use

This report is issued without limitation.

2. REFERENCES

a. TODI WG3-3-A25-TDI-0004, "North Anna 3 Maximum Ground Water Level", Revision 0
b. TODI WG3-3-A25-TDI-0007, "North Anna 3 Engineering Properties of Subsurface Material for Sliding Stability Analysis", Revision 0
c. 105E3908, "ESBWR Nuclear Island General Arrangement Drawing", Revision 5
d. 26A6642AJ, "ESBWR Design Control Document Tier 2 Chapter 3 Sections 3.1 – 3.8", Revision 10
e. 26A6642AL, "ESBWR Design Control Document Tier 2 Chapter 3 Appendices 3A – 3F", Revision 10
f. 26A6654, "ESBWR Stability Analysis of Control Building", Revision 4
g. USNRC, NUREG-0800, "Standard Review Plan for the Review of Safety Analysis Reports for Nuclear Power Plants - LWR Edition", SRP 3.8.5, "Foundations", Revision 1, July 1981
h. Tseng, W.S. and Liou, D.D., Simplified Methods for Predicting Seismic Basemat Uplift of Nuclear Power Plant Structures, Transactions of the 6th International Conference on SMIRT, Paris, France, August 1981
i. WG3-U73-ERD-S-0001, "North Anna 3 Control Building Seismic Analysis Report", Revision 0
j. TODI WG3-A25-TDI-S-0003 "North Anna 3 Rock Allowable Bearing Pressure for Lateral Loading Conditions for the RB/FB, CB & FWSC", Revision 0
k. WG3-U73-ERD-S-0005, "North Anna 3 Control Building and Reactor/Fuel Building Complex Seismic Structure-Soil-Structure Interaction Analysis Report", Revision 0
l. TODI WG3-3-A25-TDI-0005, "North Anna 3 Power Block Excavation/Backfill Drawings, Concrete Backfill Properties & Plot Plan", Revision 5
m. ACI 318-05/ACI 318R-05: Building Code Requirements for Structural Concrete (ACI 318-05) and Commentary (ACI 318R-05)
n. TODI WG3-3-A25-TDI-0006, "North Anna 3 Best Estimate Elevation of Top of Zone III Rock and Top of Zone III-IV Rock for RB/FB, CB and FWSC Structures", Revision 0
o. 26A6653, "ESBWR Control Building Structural Design Report", Revision 5

3. INPUTS

The calculations presented in this report are performed using the results obtained from the site-specific SSI analyses of the CB stand-alone model with full (uncracked concrete) stiffness properties and SSE damping values for best estimate (BE), lower bound (LB), and upper bound (UB) partial column and full column subgrade profiles (analysis Cases 7 through 12 in Table 4.2-1 of Reference 2-i). As shown in Appendix B of Reference 2-i, the

seismic response analyses of the models representing full (uncracked concrete) stiffness properties of the CB reinforced concrete structure provide conservative seismic load demands for the NA3 rock site with high frequency design motion. The use of seismic responses obtained from the model with SSE damping values for the stability evaluations is adequate because these analyses consider the limiting conditions that are associated with a high dissipation of energy in the SSI dynamic system. The consideration of different embedment configurations and subgrade profiles ensures that the stability and bearing pressure evaluations adequately capture effects of subgrade profile and dynamic property variations on the seismic response of the CB.

As described in Figure 4.3-5 and 4.3-9 Reference 2-i, 3-D contact spring elements are established in the CB model used for the site-specific SSI analyses at:

a. the interfaces between the CB exterior walls and basemat with the surrounding concrete and structural fill.

b. the interfaces between the concrete fill block supporting the CB foundation and the surrounding subgrade located at the bottom of the concrete fill block.

The SSI analyses in Reference 2-i provide spring force results from the contact spring elements located at the bottom of the CB basemat that are used as inputs to calculate the time histories of the seismic driving force and moment demands in three orthogonal directions for:

- the evaluations of the sliding stability with respect to the critical sliding plane located at the bottom of the CB basemat.

- the calculations of the dynamic bearing demand from the CB foundation on the supporting concrete fill.

The spring force results from the contact spring elements located at the interfaces between the concrete fill and the surrounding subgrade are used as inputs to calculate the time histories of the seismic driving forces used for the evaluation of the CB sliding stability with respect to the critical sliding plane located at the bottom of the concrete fill/ top of Zone III-IV rock. These calculations of the sliding stability also provide the lateral pressures on the Zone III rock that are required for the overall sliding stability of the CB and the concrete fill block supporting the building.

The site-specific groundwater elevation, friction coefficient, embedment depths and other site-specific parameters used as input for the stability and bearing pressure calculations presented in this report are shown in Table 3-1. Table 3-1 also provides the bearing and lateral load capacity of the subgrade materials at the CB location.

4. OVERTURNING STABILITY

The Factors of Safety against overturning due to earthquake loading for the CB, are determined by using the energy approach described in DCD Tier 2 Subsection 3.7.2.14 (Reference 2-d), conservatively neglecting the resistance provided by the building embedment. The overturning stability calculations use the results from the site-specific SSI analyses of the CB model with full (uncracked concrete) stiffness properties and SSE damping values (Cases 7 to 12 in Table 4.2-1 in Reference 2-i).

Seismic loads are dynamic in nature. The method of calculating seismic loads with dynamic analysis and then treating them as static loads to evaluate the overturning of structures and foundation failures while treating the foundation materials as linear elastic is conservative. Overturning of the structure, assuming no soil slip failure occurs, can be caused only by the center of gravity of the structure moving far enough horizontally to cause instability.

Furthermore, when the combined effect of the earthquake ground motion and the structural response is strong enough, the structure undergoes a rocking motion pivoting about either edge of the base. When the amplitude of the rocking motion becomes so large that the center of the structural mass reaches a position right above either edge of the base, the structure becomes unstable and may tip over. The mechanism of the rocking motion is like an inverted pendulum and its natural period is long compared with the linear, elastic dynamic structural response. Thus, with regard to overturning, the structure can be treated as a rigid body dynamic system as shown in Figure 4-1.

The maximum kinetic energy is conservatively estimated as the sum of the maximum kinetic energies of each lumped mass m_i of the CB structural model as follows:

$$E_s = \frac{1}{2}\sum_i m_i\left[(V_H)_i^2 + (V_V)_i^2\right] \qquad \text{.....(4-1)}$$

where $(V_H)_i$ and $(V_V)_i$, respectively, are the maximum calculated values of the lateral velocity and vertical velocities of the lumped mass m_i for the total duration of the input control motion.

The lumped mass velocities $(V_H)_i$ and $(V_V)_i$ are computed as follows:

$$\left|(V_H)_i\right| = \left|(V_x)_i\right| + \left|(V_H)_g\right| \text{ or } \left|(V_H)_i\right| = \left|(V_y)_i\right| + \left|(V_H)_g\right|$$
$$\left|(V_V)_i\right| = \left|(V_z)_i\right| + \left|(V_V)_g\right| \qquad \text{.....(4-2)}$$

where $(V_H)_g$ and $(V_V)_g$ are the peak horizontal and vertical ground velocity, respectively, and $(V_x)_i$, $(V_y)_i$, and $(V_z)_i$ are the maximum lateral and vertical velocities of the lumped mass m_i

relative to the ground. These maximum velocities V_x, V_y, and V_z are obtained from the results of the seismic SSI analysis and include the combination of the three earthquake components.

Letting m_0 be the total mass of the building and conservatively neglecting the effects of the building embedment, the energy required to overturn the structure is calculated as follows:

$$E_0 = m_0 gh - W_b \quad \text{.....(4-3)}$$

where, h is the height to which the center of mass of the structure has to be lifted to reach the overturning position, g is the gravity constant, and W_b is the potential energy due to groundwater buoyancy.

Figure 4-2 presents a diagram explaining the calculations of the effect of buoyancy on the energy required to overturn the structure. The stability evaluations are performed considering the NA3 site-specific nominal groundwater level specified in Table 3-1. For structures that are not symmetrical, the value of h is computed with respect to the edge of the foundation that is nearer to the building center of mass.

The Factor of Safety (FS) against overturning is defined as follows.

$$FS = \frac{E_0}{E_s} = \frac{m_0 gh - W_b}{E_s} \quad \text{.....(4-4)}$$

where,

E_0 = Energy required to overturn the structure
E_s = Maximum kinetic energy
m_0gh = Potential energy needed to lift the structure to the overturning position
W_b = Potential energy caused by buoyancy

Table 4-1 presents the calculated overturning stability Factors of Safety based on the results of the CB SSI analyses in Reference 2-i of the partial column profiles (Cases 7 through 9) and the full column profiles (Cases 10 through 12), respectively. The table shows that the CB site-specific SSI analysis of the UB partial column profile (Case 9) provides the seismic responses that are governing for the overturning stability of the CB with a minimum Factor of Safety of 519 for the overturning of the building in the EW direction without considering the beneficial effect of building foundation embedment. The calculated overturning stability Factors of Safety are much greater than the SRP 3.8.5 (Reference 2-g) Factor of Safety acceptance criteria of 1.1. Therefore, the calculations demonstrate the adequate stability of the CB against overturning.

The details of the site-specific evaluation of overturning stability of the CB are described in Appendix A.

5. SLIDING STABILITY

The site-specific evaluations of the CB sliding stability follow a methodology that is consistent with the methodology used for the standard design sliding stability evaluations in DCD Tier 2 Subsection 3.7.2.14 (Reference 2-d). In accordance with SRP 3.8.5 (Reference 2-g), the sliding evaluation is performed for two orthogonal horizontal directions separately using a linear time history analysis approach. In each direction, the phasing between the horizontal shear and vertical seismic forces is considered at each time step to compute sliding Factors of Safety (*FS(t)*) for different instances of time as the ratio between the base friction resistance and the horizontal driving force. The minimum value obtained during the duration of the site-specific ground motion is adopted as the Safety Factor for sliding stability of the CB.

The lateral resistance force demands on the surrounding embedment are computed if, at the particular instance of time, the base friction resistance alone is not sufficient to achieve a minimum Factor of Safety of 1.1 against sliding. For the instances of time when the magnitudes of these lateral resistance forces are maximum, the maximum passive lateral pressure demands on the subgrade surrounding the CB are calculated assuming that the lateral resistance against sliding is provided only by the concrete fill and the Zone III rock and conservatively neglecting the lateral resistance of the softer structural fill/ in-situ saprolite located above the Zone III rock nominal top elevation of 265 ft, NAVD 88 (standard design El.-3.12m). The maximum value of the lateral pressure demands that are required to maintain a sliding stability Factor of Safety of 1.1 is compared with the values of the allowable dynamic lateral bearing pressure of the Zone III rock provided in Reference 2-j to demonstrate that the subgrade surrounding the CB at the NA3 site has the required lateral capacity to resist sliding.

The evaluation of the CB sliding stability considers the two critical sliding failure planes located at:

a. the bottom of the CB basemat at elevation 241 ft, NAVD 88 (standard design El. -10.4 m), and

b. the bottom of the concrete fill block supporting the CB basemat at nominal elevation 225 ft, NAVD 88 (standard design El. -15.31 m).

Figure 5-1 shows a diagram of the forces considered for the stability evaluation for the CB sliding at the failure plane located at the bottom of the CB basemat. As shown in this figure, these sliding stability calculations consider the friction resistance force (F_{ub}) at the interface between the bottom of the CB basemat and the top of the supporting concrete fill as well as the lateral passive resistance (F_r) provided by the concrete fill and Zone III rock subgrade materials surrounding the CB embedded exterior walls and the CB basemat in the direction

opposite to the direction of motion. The following resistances are conservatively neglected in the sliding stability calculations:

- skin friction resistance forces acting on the vertical surfaces of the CB embedded exterior walls and basemat sides parallel to the direction of motion.
- lateral passive resistance pressure provided by the structural fill and in-situ saprolite along the face of the embedded exterior wall opposite to the direction of motion.

Figure 5-2 shows a diagram of the forces considered for the stability evaluation for sliding at the failure plane located at the bottom of the concrete fill supporting the CB foundation at the interface with the Zone III-IV rock at nominal elevation of 225 ft, NAVD 88 (standard design El. -15.31 m). These sliding stability calculations consider the friction resistance force (F_{ub}) at the bottom of the underlying concrete fill and the lateral passive resistance (F_r) provided by the surrounding concrete fill and Zone III rock. The following resistances are conservatively neglected in the sliding stability calculations:

- skin friction resistance forces acting on the vertical surfaces of the embedded exterior walls, basemat and concrete fill block sides parallel to the direction of motion.
- lateral passive resistance pressure provided by the structural fill and in-situ saprolite along the face of the embedded exterior wall opposite to the direction of motion.

The Factor of Safety for the CB structure against sliding is obtained as the minimum value of the *FS(t)* time history calculated per the:

$$FS(t) = \frac{F_{ub}(t)}{F_v(t)} \qquad \text{.....(5-1)}$$

where,

$F_v(t)$ = Time history of the horizontal driving seismic force of the embedded SSI system.

$F_{ub}(t)$ = Friction resistance force of the sliding failure plane.

The time histories of the horizontal and vertical seismic driving forces ($F_v(t)$ and $V_z(t)$) are calculated as described in Section 5.6 of Reference 2-i as the algebraic sum of the SASSI2010 spring force results at the interface nodes of the evaluated sliding failure plane and the four vertical planes extending from the sliding plane to the top of the SSI analysis model.

The friction force resisting the sliding at the sliding plane being considered is calculated as follows:

$$F_{ub}(t) = \{(D\text{-}B) - abs(V_z(t))\}\ \mu \qquad \text{.....(5–2)}$$

where,

D = Gravity force that includes:

- the seismic weight of the CB assigned to the CB dynamic model that includes the building dead weight and 25% of the live loads.
- the weight of the concrete fill above the sliding plane, if applicable.

B = Buoyancy force based on the site-specific nominal groundwater El. 281.0 ft NAVD88 (standard design El. 1.76m) at the CB location per Reference 2-a, which is 2.74 m (9 ft) below finished ground level grade located at El. 290 ft NAVD88 (standard design El. 4.5m).

$V_z(t)$ = Vertical seismic force time history of the embedded SSI system (both positive and negative directions of the vertical base reaction are considered in the calculations).

μ = Coefficient of friction at the sliding plane interface.

The evaluations of the CB sliding stability for both sliding planes being considered use one value of friction coefficient $\mu=0.6$, which is the lowest of those specified in Reference 2-b for the concrete fill and rock interfaces. Due to the high stiffness of the fill concrete and Zone III rock surrounding the CB, small deformations are needed to engage the required lateral resistance of the concrete fill/rock strata with no relative motion occurring at the sliding failure planes.

If at the particular instance of time the base friction resistance (F_{ub}) alone is not sufficient to achieve a minimum Factor of Safety of 1.1 against sliding, the lateral resistance force (F_r) at the vertical plane opposite to the direction of motion is calculated as follows:

$$F_r = 1.1F_v - F_{ub} \qquad \text{.....(5-3)}$$

The maximum passive lateral pressure demands on the subgrade surrounding the CB are calculated for the instance of time when the maximum lateral resistance force (F_r) is required for achieving the Factor of Safety against sliding of 1.1. The passive lateral pressure calculations assume that the lateral resistance against sliding is provided only by the concrete fill and the Zone III rock. The lateral resistance provided by the 7.62 m (25 ft) deep stratum of softer structural fill and in-situ saprolite located above the Zone III rock is conservatively neglected. A triangular lateral passive pressure distribution is assumed, as shown in Figures 5-1 and 5-2, to conservatively calculate the maximum lateral passive pressure demand on the subgrade surrounding the CB.

Appendix B presents plots of the time histories of the total vertical base reaction force and the horizontal seismic forces in the NS and EW directions used for the CB sliding stability calculations. The instances of time that are critical for the sliding stability of the CB in the

EW and NS directions and yield maximum values of required lateral passive pressures on the subgrade are identified in these plots.

Table 5-1 presents the calculations of the CB sliding stability with respect to the critical sliding plane located at the bottom of the basemat. These calculations account for the friction resistance force at the bottom of the basemat and the lateral resistance pressure provided by the embedded exterior wall and basemat to resist the horizontal seismic load while maintaining a Factor of Safety greater than 1.1.

The results for the maximum lateral resistance pressure for each of the six SSI analyses cases presented in Tables 5-1 and 5-2 show that the SSI analysis of the UB partial column profile (Case 9 in Table 4.2-1 of Reference 2-i) provides the maximum lateral pressure demands on the subgrade at the bottom of the CB basemat. The evaluations of the CB stability against sliding in the EW direction for this critical SSI analysis case show that the maximum lateral pressure demand on the subgrade that is required to maintain a Factor of Safety of 1.1 for the sliding stability of the CB will not be greater than 1.17 MPa. This value is below the value of 1.39 MPa specified in Table 3-1 as the allowable lateral bearing pressure of the concrete fill and rock subgrade at the CB basemat elevation 241 ft, NAVD 88 (standard design El. -10.4 m). Figures 7-1 through 7-8 present the site-specific lateral pressure demands on the embedded exterior walls of the CB at column lines CA and CD and show that the magnitudes of the passive pressures required for the sliding stability of the CB are comparable with the magnitudes of the dynamic lateral pressures developed from the SSI analyses results as described in Section 5.5 of Reference 2-i. The results of the SSI analyses indicate that these dynamic lateral pressures are associated with very small lateral deformations of the subgrade surrounding the CB at the NA3 site. Table 6.2-1 of Reference 2-i shows that the maximum lateral displacements of the CB at the plant grade elevation relative to the free-field motion are very small (less than 2.4 mm). The maximum lateral displacements of the portion of the CB that is embedded in the Zone III rock, which has a top El. 265 ft, NAVD 88 (standard design El. -3.12 m), are even smaller (less than 0.7 mm). Therefore, the displacements associated with the passive lateral pressures obtained from the sliding evaluations presented in this report will also be very small and will not result in relative motion between the CB basemat and the supporting concrete fill.

Table 5-2 presents the calculations of the sliding stability with respect to the critical sliding plane at the interface between the concrete fill and the Zone III-IV rock surface located at a nominal elevation of 225 ft, NAVD 88 (standard design El. -15.31 m). These calculations consider the friction resistance force at the bottom of the concrete fill and the lateral passive pressure resistance of the surrounding Zone III rock to maintain a Factor of Safety greater than 1.1. The last row of Table 5-2 shows that the maximum lateral resistance pressure needed to achieve the required sliding stability Factor of Safety of 1.1 is no greater than 0.74 MPa, which is considerably less than 1.47 MPa specified in Table 3-1 as the allowable lateral bearing pressure of the rock at elevation 225 ft, NAVD 88 (standard design El. -15.31 m).

This maximum lateral pressure demand on the Zone III rock at the bottom of the concrete fill is obtained from the calculations of the sliding stability in the NS direction for the SSI analysis of the UB partial column profile. Additional evaluations of the capacity of the concrete fill block, placed between the CB and the RB/FB, to withstand the lateral load demands from these two buildings is described in Reference 2-k. These evaluations are based on the results of the site-specific structure-soil-structure (SSSI) analyses of the CB-RB/FB combined model that provide an explicit representation of the subgrade conditions between the two buildings.

The site-specific sliding stability calculations presented in this section demonstrate that the CB will maintain the stability against sliding at the two critical sliding failure planes located at the bottom of the CB basemat and at the bottom of the concrete fill supporting the CB foundation. The maximum lateral pressures required to maintain a sliding Factor of Safety that is greater than the SRP 3.8.5 (Reference 2-g) Factor of Safety acceptance criteria of 1.1 are less than the lateral bearing capacity of the subgrade surrounding the CB. The maximum required lateral pressures calculated in this section are used as inputs for the site-specific evaluations of the CB structure to demonstrate that the capacity of the CB below-grade walls is sufficient to resist these lateral passive resistance pressure demands.

6. DYNAMIC BEARING PRESSURES

The maximum site-specific dynamic bearing pressure demands on the concrete fill supporting the CB foundation and the underlying Zone III-IV rock are evaluated using the EB/MEB method, as described in Reference 2-h, that is also used for the standard design bearing pressure evaluations in Reference 2-f. The basemat uplift rotation, moment, and foundation bearing pressures are calculated in accordance with the MEB method using the SASSI2010 analysis results for the spring forces at the bottom of the CB basemat obtained from the SSI analyses of the CB model with full (uncracked concrete) stiffness properties and SSE damping values for the LB, BE and UB partial and full column profiles (Cases 7 through 12 in Table 4.2-1 in Reference 2-i).

The time histories of the vertical base reactions are calculated by summing up the nodal spring forces:

- at the bottom of the CB basemat to calculate the dynamic bearing pressure demand on the underlying concrete fill, and
- at the bottom of the underlying concrete fill to calculate the dynamic bearing pressure demand on the Zone III-IV rock

The evaluation of the dynamic bearing pressure under the CB basemat considers the seismic weight of the CB that includes the building self-weight and 25% of the design live loads. The evaluation of the dynamic bearing pressure on the Zone III-IV rock considers, in addition of

the CB seismic weight, the weight of the approximately 5 m (16 ft) thick layer of concrete fill placed between the CB foundation and the Zone III-IV rock surface. Two calculations are performed for each of the six SSI analysis cases considering the upward and downward direction of the vertical seismic force. In order to capture the effect of the groundwater on the dynamic bearing pressure calculations, the buoyancy force is subtracted from the gravity force for the calculations that consider upward seismic force.

The time histories of the overturning moments about the X and Y axes of the foundation are calculated for both directions by summing the moments generated by each nodal spring reaction. The same approach is used to calculate the dynamic bearing pressure demands on the Zone III-IV rock that are transferred on the NA3 rock through the layer of concrete fill.

Appendix B presents plots of the total vertical load and the overturning moment time histories obtained from the set of six site-specific CB SSI analyses Cases 7 through 12 described in Table 4.2-1 of Reference 2-i. These plots identify the critical instances of time (when the combined vertical load and overturning moment time histories attain the maximum absolute values) used for the calculation of the maximum dynamic bearing pressures in Tables 6-1 and 6-2.

The evaluation of the maximum dynamic bearing pressure on the concrete fill supporting the CB basemat considers a vertical gravity load with a magnitude equal to the seismic weight of the CB (weight assigned to the CB dynamic model) that includes the building dead weight and 25% of the design live loads. The evaluation of the maximum bearing pressure demands on the NA3 in-situ rock also considers the weight of the concrete fill placed between the CB basemat and the Zone III-IV rock located at nominal elevations of 241 ft and 225 ft, NAVD 88 (standard design El. -10.4m and El. -15.31m), respectively.

Table 6-1 presents the calculations of the maximum dynamic bearing pressures from the CB basemat on the underlying concrete fill for each one of the six SSI analyses Cases 7 through 12 in Table 4.2-1 of Reference 2-i. The table shows that the calculations for the UB partial column profile (Case 9) yield a bounding maximum toe bearing pressure demand of 1.46 MPa (30.5 ksf) which is lower than the maximum toe bearing pressure demand of 2.19 MPa (45.7 ksf) considered by the standard design (Reference 2-f, Table 7-1). This maximum site-specific dynamic bearing pressure demand is also considerably lower than the allowable dynamic pressure of 8.0 MPa (167 ksf) specified in Sections 9.3.5 and 22.5.5 of ACI 318-05 (Reference 2-m) for concrete fill material with a compressive strength of 2,500 psi as provided in Reference 2-l.

Table 6-2 presents the calculations of the maximum dynamic bearing pressures on the surface of the underlying Zone III-IV rock for each one of the six SSI analyses Cases 7 through 12 described in Table 4.2-1 of Reference 2-i. The table shows that the maximum bearing pressure demand on the in-situ rock is 0.73 MPa (15.2 ksf) which is considerably

lower than 12.4 MPa (259 ksf) specified in Reference 2-b for the allowable dynamic bearing pressure of the Zone III-IV rock.

7. LATERAL PRESSURES

Figure 7-1 through Figure 7-8 provide plots of the NA3 site-specific total lateral soil pressures acting on the below grade exterior walls of CB. Two plots are provided in each figure. The first plot shows the distributions of the static and the dynamic components of the active lateral pressures acting on the walls. The distribution of the static pressure (p_s) that includes the at-rest static soil pressure and the hydrostatic pressure from the groundwater are calculated as follows using the NA3 site-specific values of the at-rest soil coefficients (K_0) and the groundwater level depth (h_w) provided in Table 3-1:

for $z = 0$ to h_w $\quad p_s = K_0^s \cdot \left(\gamma_s^{dry} \cdot z + q_s\right)$

for $z = h_w$ to h_r $\quad p_s = K_0^s \cdot \left(\gamma_s^b \cdot (z - h_w) + \gamma_s^{dry} \cdot h_w + q_s\right) + \gamma_w \cdot \left(z - h_w\right)$ .....(7–1)

for $z > h_r$ $\quad p_s = K_0^r \cdot \left(\gamma_c^b \cdot (z - h_r) + \gamma_s^b \cdot \left(h_r - h_w\right) + \gamma_s^{dry} \cdot h_w + q_s\right) + \gamma_w \cdot \left(z - h_w\right)$

where: z is the depth coordinate,

h_r and h_w are the nominal depth of the Zone III rock and groundwater,

q_s is the surcharge surface pressure per Appendix B of Reference 2-o,

γ_w is the unit weight of water,

K_0^s, γ_s^{dry} and γ_s^b are the at-rest coefficient, the dry and submerged unit weight of the structural fill,

K_0^r and γ_c^b are the at-rest coefficient and the submerged unit weight of the concrete fill.

The at-rest coefficient of the concrete fill is calculated using the concrete fill Poisson ratio ν_c and the following formula from the theory of elasticity:

$$K_0^r = \frac{\nu_c}{1 - \nu_c} \qquad \text{.....(7–2)}$$

The dynamic pressure distributions are developed based on the SSI analysis results for horizontal forces of the contact springs located at the wall-subgrade interfaces as described in in Section 5.5 of Reference 2-i. Figures 7-1 through 7-8 present the envelope of the lateral pressure results obtained from the SSI analyses of the LB, BE and UB subgrade profiles. The site-specific static and dynamic lateral pressure demands are compared with the

corresponding static and dynamic lateral pressure loads used for the standard design of the CB.

Figure 7-1 through Figure 7-8 show that near the slab at El. 267.9 ft., NAVD88 (standard design El. -2.25 m) and near the top of the CB basemat at El. 251.0 ft., NAVD88 (standard design El. -7.40 m), the site-specific total lateral pressures can exceed the total lateral pressures used for the standard design of CB structures. Figures 7-3 and 7-4 also show that the lateral passive pressures required to ensure the stability of the CB against sliding in the EW direction can also exceed the pressures used for the standard design for the CB wall capacity check.

Therefore, the site-specific CB structural evaluation will be performed to demonstrate that the wall pressure capacity of the standard design of the CB structure is adequate to withstand the NA3 site-specific lateral pressure demands on the CB below-grade exterior walls.

8. CONCLUSIONS

The site-specific stability evaluations presented in this report demonstrate that the site-specific minimum Factors of Safety for overturning and sliding of the CB at the NA3 site are all greater than the Factors of Safety specified by SRP 3.8.5 (Reference 2-g).

The site-specific stability evaluations that conservatively neglect the resistance of the CB embedment show that the Factors of Safety against the CB overturning are much greater than the SRP 3.8.5 (Reference 2-g) Factor of Safety acceptance criteria of 1.1.

The sliding stability evaluations demonstrate that base friction and the lateral resistance provided by the concrete fill and Zone III rock embedment alone are sufficient to resist the seismic driving forces and ensure that the CB maintains a Factor of Safety against sliding that is greater than the required Factor of Safety of 1.1 in SRP 3.8.5 (Reference 2-g). The site-specific sliding stability calculations demonstrate that the CB will maintain the stability against sliding at the two critical sliding failure planes located at the bottom of the CB basemat and the bottom of the concrete fill supporting the CB foundation. The maximum lateral pressures required to maintain a sliding Factor of Safety greater than 1.1 are less than the lateral bearing capacity of the subgrade surrounding the CB. The maximum required lateral pressures together with the total lateral pressures presented in this report are used as input for the site-specific evaluations of the CB structure to demonstrate that the capacity of the CB below-grade exterior walls is sufficient to resist these site-specific lateral pressure demands.

The site-specific dynamic foundation bearing pressure calculations presented in this report show that the NA3 site-specific demands are lower than the dynamic bearing pressures considered in the standard design of the CB. The calculated maximum dynamic pressures are

also lower than the allowable bearing pressure of the concrete fill supporting the CB basemat and the allowable bearing pressure of the underlying NA3 Zone III-IV rock subgrade.

Table 3-1: Site-Specific Parameters

Parameters	Values	Reference
Building Width:		
X-direction (NS-direction)	30.3 m(99.4ft)	2-c
Y-direction (EW-direction)	23.8 m(78.1ft)	
Zone III Rock Embedment Depth:		
Nominal Zone III Rock Elevation	El. 265 ft, NAVD 88	2-n
Depth to bottom of CB basemat	7.28 m (23.9 ft)	2-i
Depth to bottom of concrete fill	12.19 m (40 ft)	
Water Level:		
Nominal Groundwater Elevation	El. 281.0 ft NAVD88 2.74 m (9 ft) below finished ground level grade	2-a
Friction Coefficient, μ:		
Foundation/Concrete Fill/Rock Interfaces	0.6*)	2-b
Allowable Lateral Dynamic Bearing Pressure:		
Zone III rock at El. 241 ft, NAVD 88	1.39 MPa (29.1 ksf)	2-j
Zone III rock at El. 225 ft, NAVD 88	1.47 MPa (30.6 ksf)	
Allowable Dynamic Bearing Pressure:		
Zone III-IV rock	12.4 MPa (259 ksf)	2-b

*) A value of 0.6 is used for the friction coefficient, which is the lowest value specified in Reference 2-b for concrete fill and Zone III-IV rock interfaces with the foundation structural concrete Table 4-1.

Table 4-1: CB Overturning Stability Evaluation

Subgrade Condition	Partial Column Profiles						Full Column Profiles					
	LB (Case 7)		BE (Case 8)		UB (Case 9)		LB (Case 10)		BE (Case 11)		UB (Case 12)	
Direction	NS	EW	NS	EW	NS	EW	NS	EW	NS	EW	NS	EW
m_0gh (MN·m)	1,525	1,028	1,525	1,028	1,525	1,028	1,525	1,028	1,525	1,028	1,525	1,028
W_b (MN·m)	123.9	131.7	123.9	131.7	123.9	131.7	123.9	131.7	123.9	131.7	123.9	131.7
E_s (MN·m)	1.3	1.2	1.5	1.5	1.9	1.7	1.2	1.1	1.3	1.2	1.5	1.4
$FS=(m_0gh-W_b)/E_s$	1,065	763	910	605	750	**519**	1,159	783	1,065	760	909	662

Note:

m_0 = total mass of structure and basemat
g = acceleration due to gravity
h = height of the center of structure mass at the overturning position
W_b = potential energy caused by the effect of buoyancy
E_s = maximum kinetic energy
FS = Factor of Safety

The red number is the minimum Factor of Safety against overturning.

Table 5-1: Evaluation of CB Stability for Sliding at Bottom of Basemat (El. 241 ft NAVD 88)

Basemat width in NS Dir.	30.3	m
Basemat width in EW Dir.	23.8	m
Depth of Zone III rock embedment	7.28	m
Total Weight	197	MN
Buoyancy	86	MN

Subgrade Condition	Partial Column Profiles						Full Column Profiles					
	LB (Case 7)		BE (Case 8)		UB (Case 9)		LB (Case 10)		BE (Case 11)		UB (Case 12)	
Sliding Direction	NS	EW	NS	EW	NS	EW	NS	EW	NS	EW	NS	EW
Time (sec)	3.090	1.810	4.630	1.810	1.070	1.805	1.065	1.810	3.085	1.805	3.085	1.805
Vertical Seismic Load (MN)	49	103	77	114	70	105	55	85	42	75	49	77
Minimum Vertical Load (MN)	62	8	34	0	41	6	56	26	69	36	62	34
F_v: Horizontal Seismic Force (MN)	61	44	71	84	104	120	50	43	60	52	93	67
F_{ub}: Bottom Friction Force (MN)	37	5	20	0	25	3	33	16	41	21	37	20
F_r: Lateral Resistance Force (MN)	30	44	58	92	90	129	22	31	24	36	65	53
FS (=$(F_{ub}+F_r)/F_v$)	1.10	1.10	1.10	1.10	1.10	1.10	1.10	1.10	1.10	1.10	1.10	1.10
σ_{max}: Maximum Stress (MPa) Associated with Lateral Resistance F_r	0.35	0.40	0.67	0.84	1.04	**1.17**	0.25	0.28	0.28	0.33	0.75	0.48

Note: The red number is the maximum lateral pressure demand on Zone III rock.

Table 5-2: Evaluation of CB Stability for Sliding at Bottom of Concrete Fill (El. 225 ft, NAVD 88)

Basemat width in NS Dir.	30.3	m
Basemat width in EW Dir.	23.8	m
Depth of Zone III rock embedment	12.38	m
Total Weight	278	MN
Buoyancy	121	MN

Subgrade Condition	Partial Column Profiles						Full Column Profiles					
	LB (Case 7)		BE (Case 8)		UB (Case 9)		LB (Case 10)		BE (Case 11)		UB (Case 12)	
Sliding Direction	NS	EW	NS	EW	NS	EW	NS	EW	NS	EW	NS	EW
Time (sec)	1.135	1.805	3.085	1.805	3.085	1.805	1.065	1.810	3.085	1.805	3.085	1.805
Vertical Seismic Load (MN)	103	125	62	133	64	145	55	85	42	75	49	77
Minimum Vertical Load (MN)	54	32	95	24	93	12	56	26	69	36	62	34
F_v: Horizontal Seismic Force (MN)	65	42	113	89	146	130	50	43	60	52	93	67
F_{ub}: Bottom Friction Force (MN)	32	19	57	14	56	7	33	16	41	21	37	20
F_r: Lateral Resistance Force (MN)	39	27	68	83	105	136	22	31	24	36	65	53
FS ($=(F_{ub}+F_r)/F_v$)	1.10	1.10	1.10	1.10	1.10	1.10	1.10	1.10	1.10	1.10	1.10	1.10
σ_{max}: Maximum Stress (MPa) Associated with Lateral Resistance F_r	0.27	0.15	0.47	0.45	0.72	**0.74**	0.15	0.17	0.16	0.19	0.44	0.28

Note: The red number is the maximum lateral pressure demand on Zone III rock.

Table 6-1: Calculations of Dynamic Bearing Pressure Demands on Concrete Fill under CB Basemat

Basemat width in NS (x) Dir.			30.3 m											
Basemat width in EW (y) Dir.			23.8 m											
Gravity Load (D)			197 MN											
Buoyancy (B)			86 MN (considered only in combination with upward vertical seismic load (V_z))											
Subgrade Condition			Partial Column Analyses						Full Column Analyses					
			LB (Case 7)		BE (Case 8)		UB (Case 9)		LB (Case 10)		BE (Case 11)		UB (Case 12)	
Direction Vertical Seismic Load			downward		upward		upward		downward		upward		upward	
SASSI	Time	(sec)	3.085		1.810		1.810		1.810		1.810		1.815	
	Vertical seismic load (V_z)	(MN)	35.7		82.5		86.8		79.8		83.2		85.1	
	Total vertical load	(MN)	233		28		24		277		280		282	
	Moment in NS-dir (Mx)	(MN-m)	590		194		172		76		152		105	
	Moment in EW-dir (My)	(MN-m)	302		528		692		218		140		69	
Simplified Method**			EB	MEB	EB	MEB	EB	MEB	EB	MEB	EB	MEB	EB	MEB
NS dir. ↓ EW dir.	Max. basemat uplift ratio α	(%)	0.0	0.0	15.5	18.2	17.6	21.0	0.0	0.0	0.0	0.0	0.0	0.0
	Max. basemat rotation (ϕ)	(10^{-4} rad)	0.004	0.004	0.002	0.002	0.001	0.001	0.010	0.010	0.009	0.009	0.005	0.005
	Max. basemat moment (Mx)	(MN-m)	590	590	194	196	172	173	76	76	152	152	105	105
	Max. bearing pressure 1 (Px)	(MPa)	0.48	0.48	0.09	0.10	0.08	0.08	0.40	0.40	0.43	0.43	0.42	0.42
	Max. bearing pressure 2 (Py)	(MPa)	---	0.11	---	0.23	---	0.31	---	0.08	---	0.05	---	0.02
	Max. Bearing pressure (Pxy=Px+Py)	(MPa)	---	0.59	---	0.32	---	0.39	---	0.48	---	0.48	---	0.44
EW dir. ↓ NS dir.	Max. basemat uplift ratio α	(%)	0.0	0.0	67.3	83.6	77.8	92.2	0.0	0.0	0.0	0.0	0.0	0.0
	Max. basemat rotation (ϕ)	(10^{-4} rad)	0.008	0.008	0.014	0.057	0.020	0.156	0.011	0.011	0.015	0.015	0.009	0.009
	Max. basemat moment (My)	(MN-m)	302	302	528	301	692	273	218	218	140	140	69	69
	Max. bearing pressure 1(Py)	(MPa)	0.43	0.43	0.22	0.48	0.28	0.85	0.46	0.46	0.44	0.44	0.42	0.42
	Max. bearing pressure 2 (Px)	(MPa)	---	0.16	---	0.33	---	0.60	---	0.02	---	0.04	---	0.03
	Max. Pressure (Pyx=Py+Px)	(MPa)	---	0.59	---	0.81	---	1.46	---	0.48	---	0.48	---	0.44
	Envelope of Pxy and Pyx	(MPa)	---	0.59	---	0.81	---	**1.46**	---	0.48	---	0.48	---	0.44

Note *: SASSI2010 analysis is a linear time history analysis with the 3D excitation.

**: EB and MEB stand for energy balance (EB) and modified energy balance (MEB) methods (Reference 2-h).

The red number is the maximum dynamic toe bearing pressure demand on the underlying concrete fill.

Table 6-2: Calculations of Dynamic Bearing Pressure Demands on Zone III-IV Rock

Basemat width in NS (x) Dir.			30.3 m											
Basemat width in EW (y) Dir.			23.8 m											
Gravity Load (D)			278 MN											
Buoyancy (B)			121 MN	(considered only in combination with upward vertical seismic load (V_z))										
Subgrade Condition			Partial Column Analyses						Full Column Analyses					
			LB (Case 7)		BE (Case 8)		UB (Case 9)		LB (Case 10)		BE (Case 11)		UB (Case 12)	
Direction Vertical Seismic Load			downward		downward		downward		downward		downward		downward	
SASSI	Time	(sec)	1.810		1.815		1.810		3.020		1.805		1.810	
	Vertical seismic load (V_z)	(MN)	114.1		112.3		122.3		16.9		106.1		121.0	
	Total vertical load	(MN)	392		390		400		294		384		399	
	Moment in NS-dir (Mx)	(MN-m)	95		144		154		314		83		13	
	Moment in EW-dir (My)	(MN-m)	177		353		380		378		251		169	
Simplified Method**			EB	MEB	EB	MEB	EB	MEB	EB	MEB	EB	MEB	EB	MEB
NS dir. ↓ EW dir.	Max. basemat uplift ratio α	(%)	0.0	0.0	0.0	0.0	0.0	0.0	0.0	0.0	0.0	0.0	0.0	0.0
	Max. basemat rotation (ϕ)	(10^{-4} rad)	-0.004	-0.004	-0.010	-0.010	-0.006	-0.006	0.006	0.006	0.005	0.005	0.002	0.002
	Max. basemat moment (Mx)	(MN-m)	95	95	144	144	154	154	314	314	83	83	13	13
	Max. bearing pressure 1 (Px)	(MPa)	0.57	0.57	0.58	0.58	0.60	0.60	0.49	0.49	0.55	0.55	0.56	0.56
	Max. bearing pressure 2 (Py)	(MPa)	---	0.06	---	0.12	---	0.13	---	0.13	---	0.09	---	0.06
	Max. Bearing pressure (Pxy=Px+Py)	(MPa)	---	0.63	---	0.70	---	0.73	---	0.63	---	0.64	---	0.62
EW dir. ↓ NS dir.	Max. basemat uplift ratio α	(%)	0.0	0.0	0.0	0.0	0.0	0.0	0.0	0.0	0.0	0.0	0.0	0.0
	Max. basemat rotation (ϕ)	(10^{-4} rad)	-0.016	-0.016	-0.008	-0.008	-0.008	-0.008	0.008	0.008	0.003	0.003	0.002	0.002
	Max. basemat moment (My)	(MN-m)	177	177	353	353	380	380	378	378	251	251	169	169
	Max. bearing pressure 1(Py)	(MPa)	0.61	0.61	0.66	0.66	0.69	0.69	0.54	0.54	0.62	0.62	0.61	0.61
	Max. bearing pressure 2 (Px)	(MPa)	---	0.03	---	0.04	---	0.04	---	0.09	---	0.02	---	0.00
	Max. Pressure (Pyx=Py+Px)	(MPa)	---	0.63	---	0.70	---	0.73	---	0.63	---	0.64	---	0.62
	Envelope of Pxy and Pyx	(MPa)	---	0.63	---	0.70	---	**0.73**	---	0.63	---	0.64	---	0.62

Note *: SASSI2010 analysis is a linear time history analysis with the 3D excitation.

**: EB and MEB stand for energy balance (EB) and modified energy balance (MEB) methods (Reference 2-h).

The red number is the maximum dynamic toe bearing pressure demand on the underlying concrete fill.

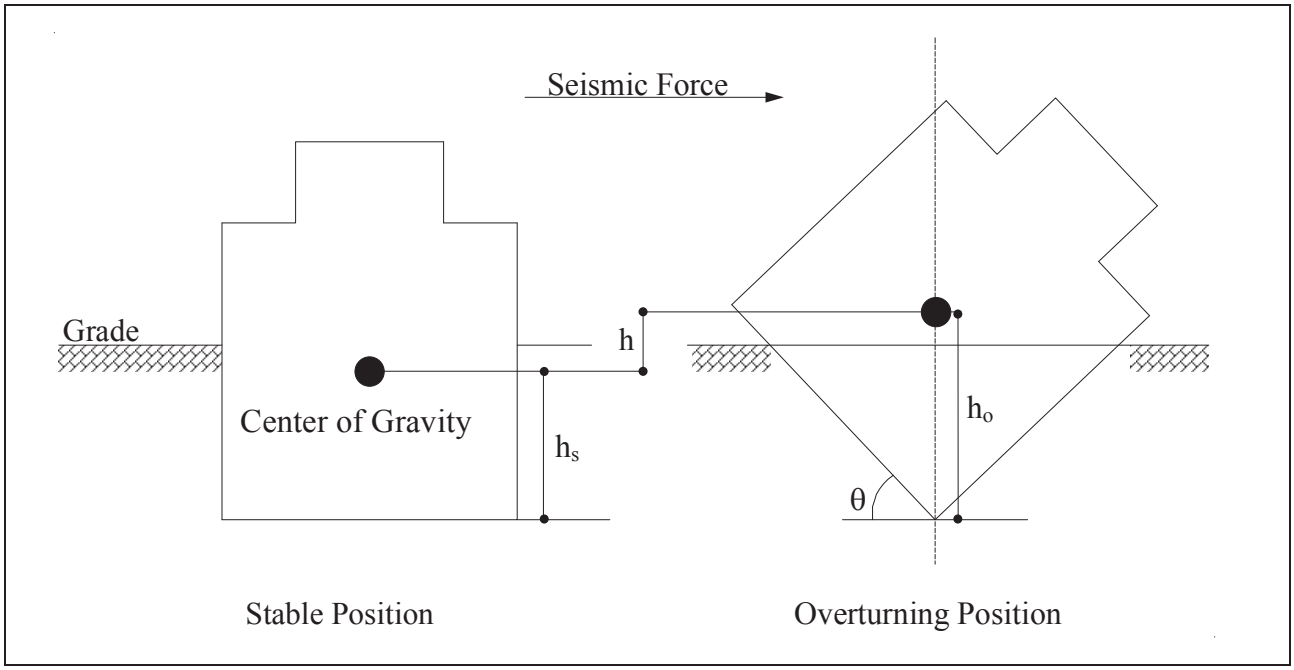

Figure 4-1: Overturning Position of Structure

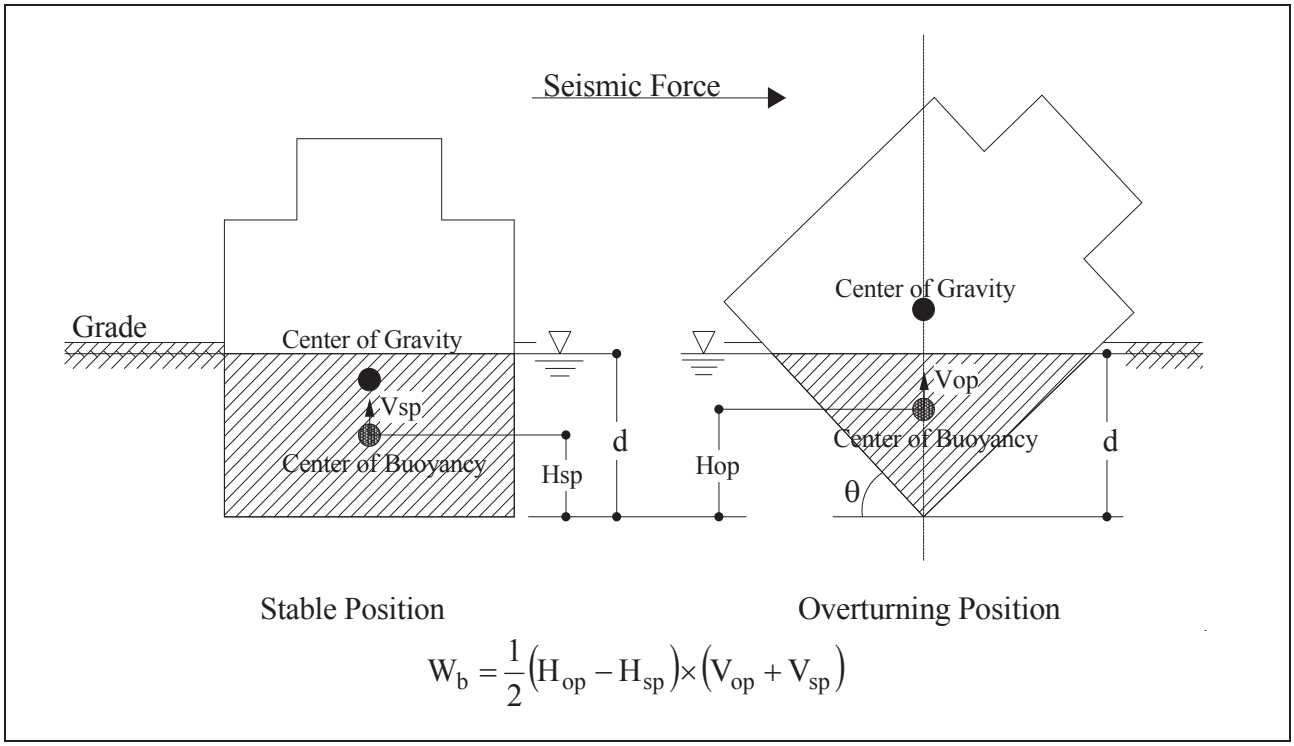

$$W_b = \frac{1}{2}\left(H_{op} - H_{sp}\right) \times \left(V_{op} + V_{sp}\right)$$

Figure 4-2: Buoyancy Effect

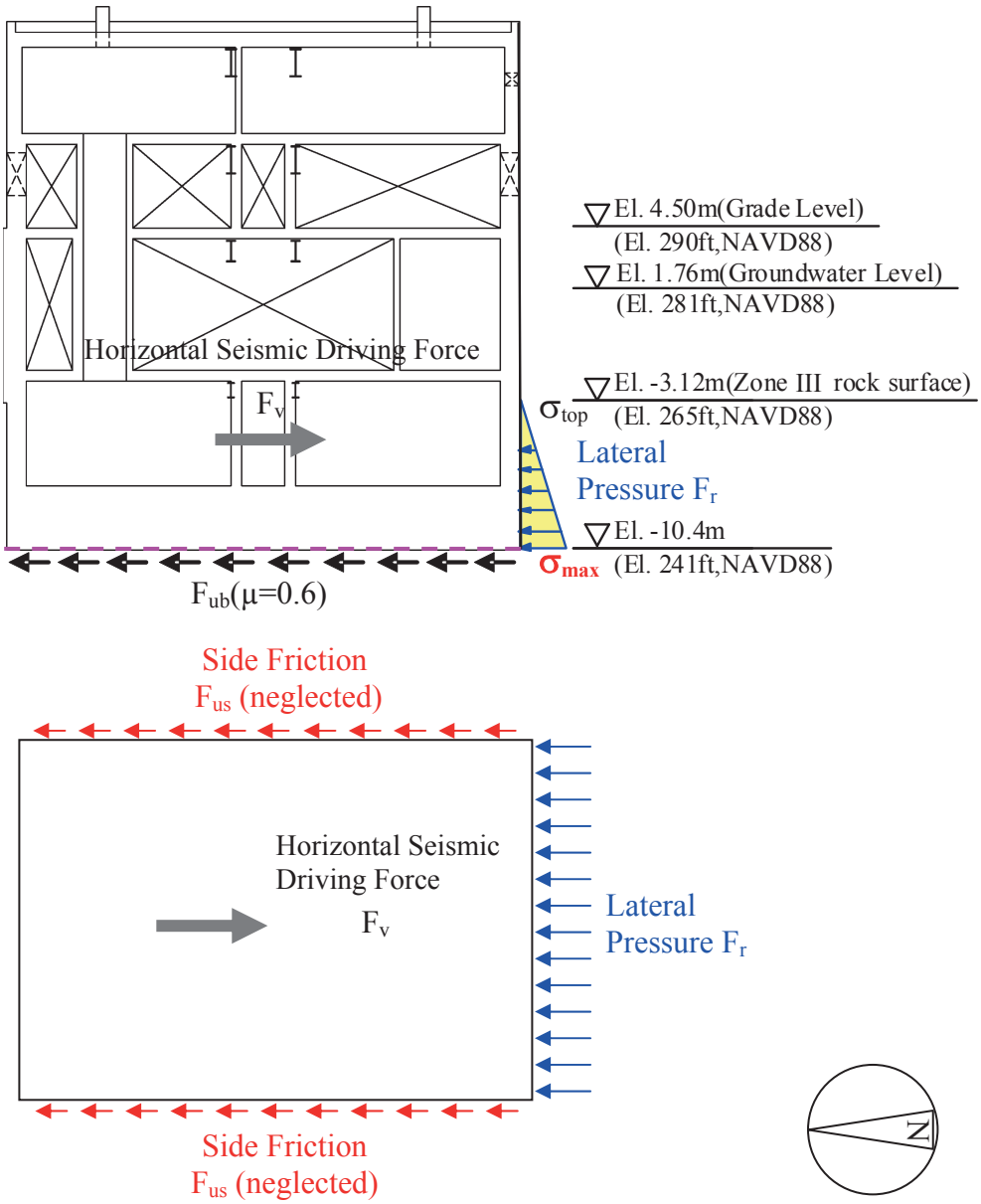

Figure 5-1: Forces for Evaluation of CB Sliding at Bottom of Basemat

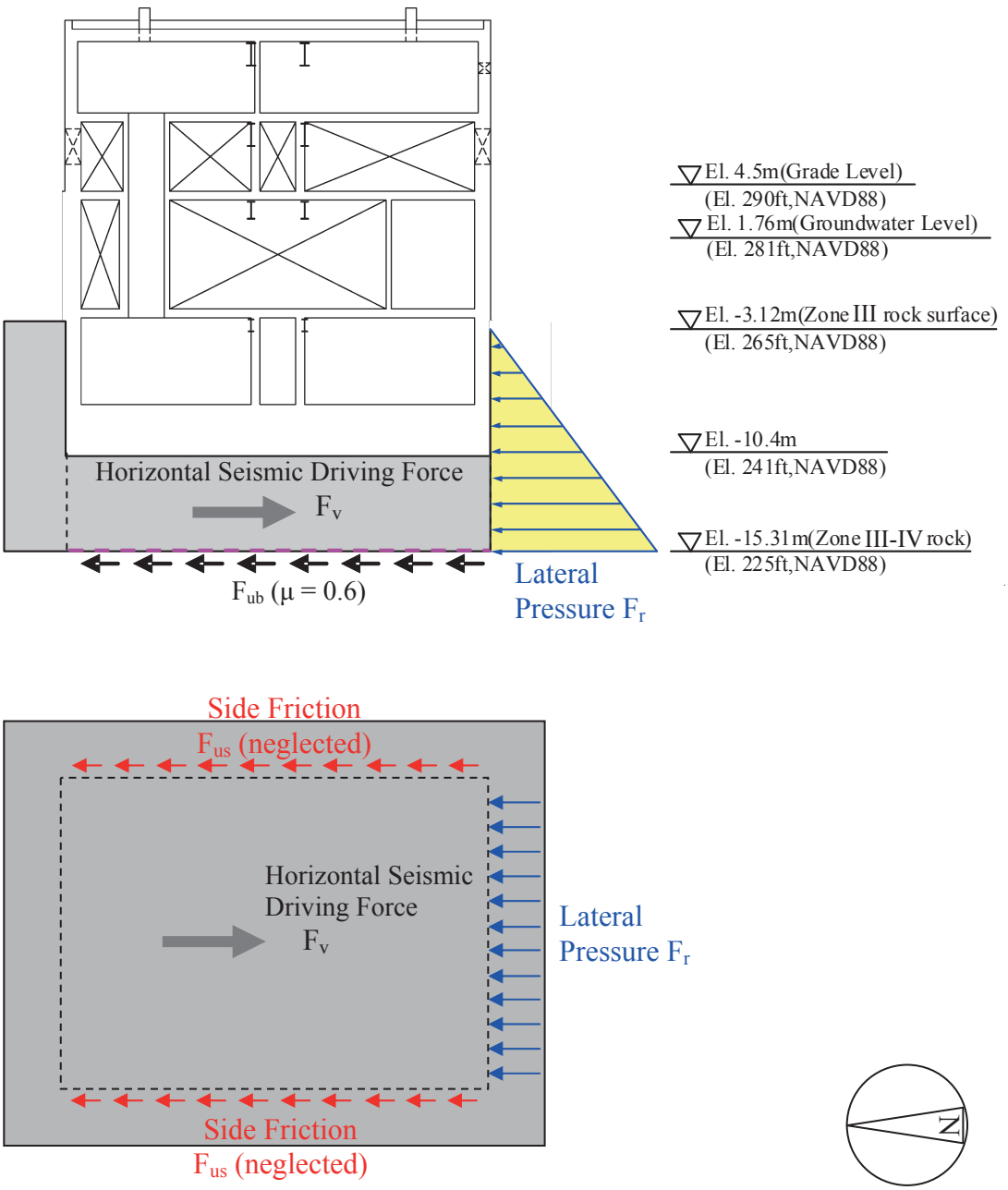

Figure 5-2: Forces for Evaluation of CB Sliding at Bottom of Concrete Fill

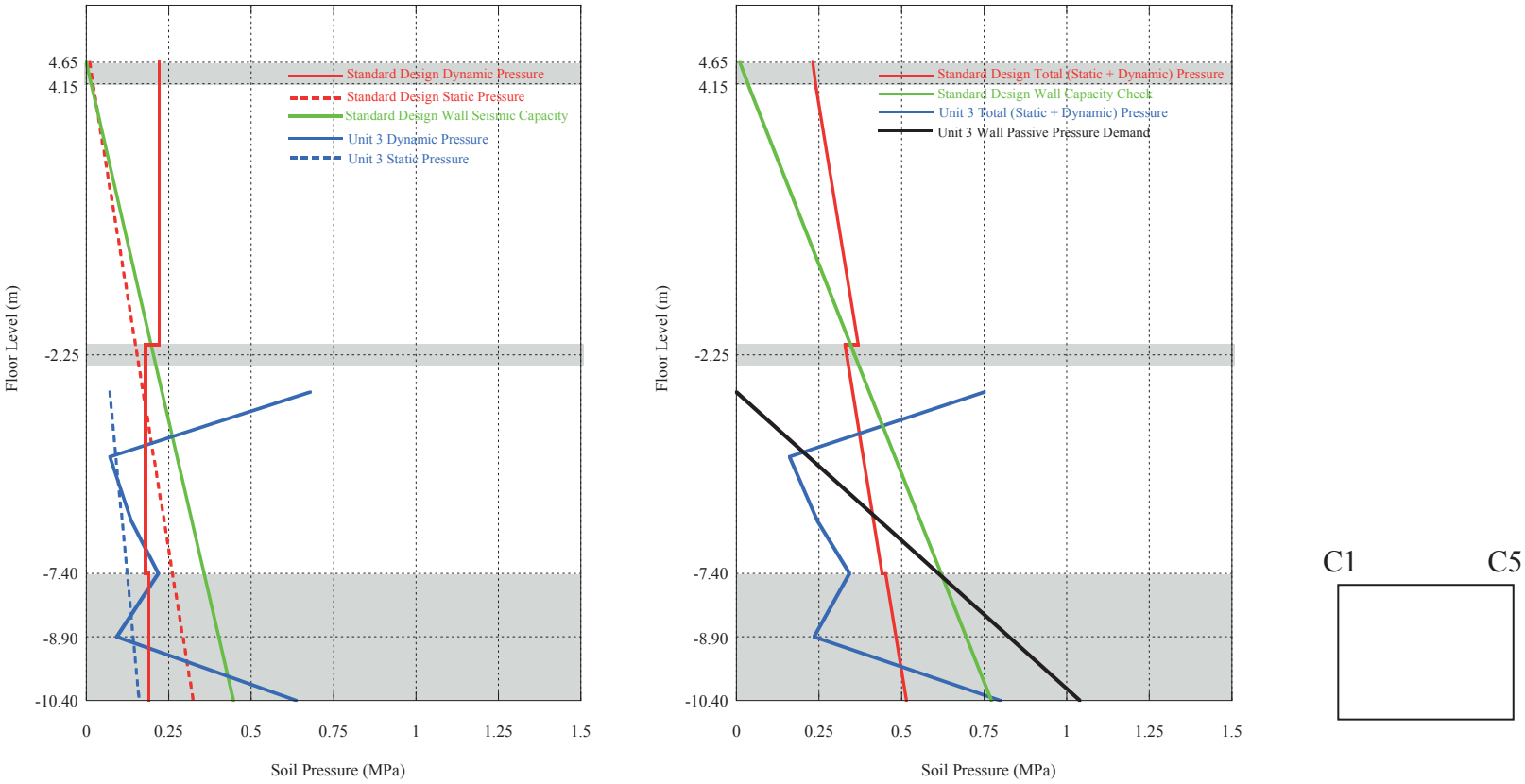

(a) Static Pressure and Dynamic Pressure **(b) Total Pressure and Wall Passive Pressure**

Note: The shaded area shows thickness of the floor slabs and basemat.

Figure 7-1: Lateral Pressure C1 Wall (Partial Column, SSE Envelope)

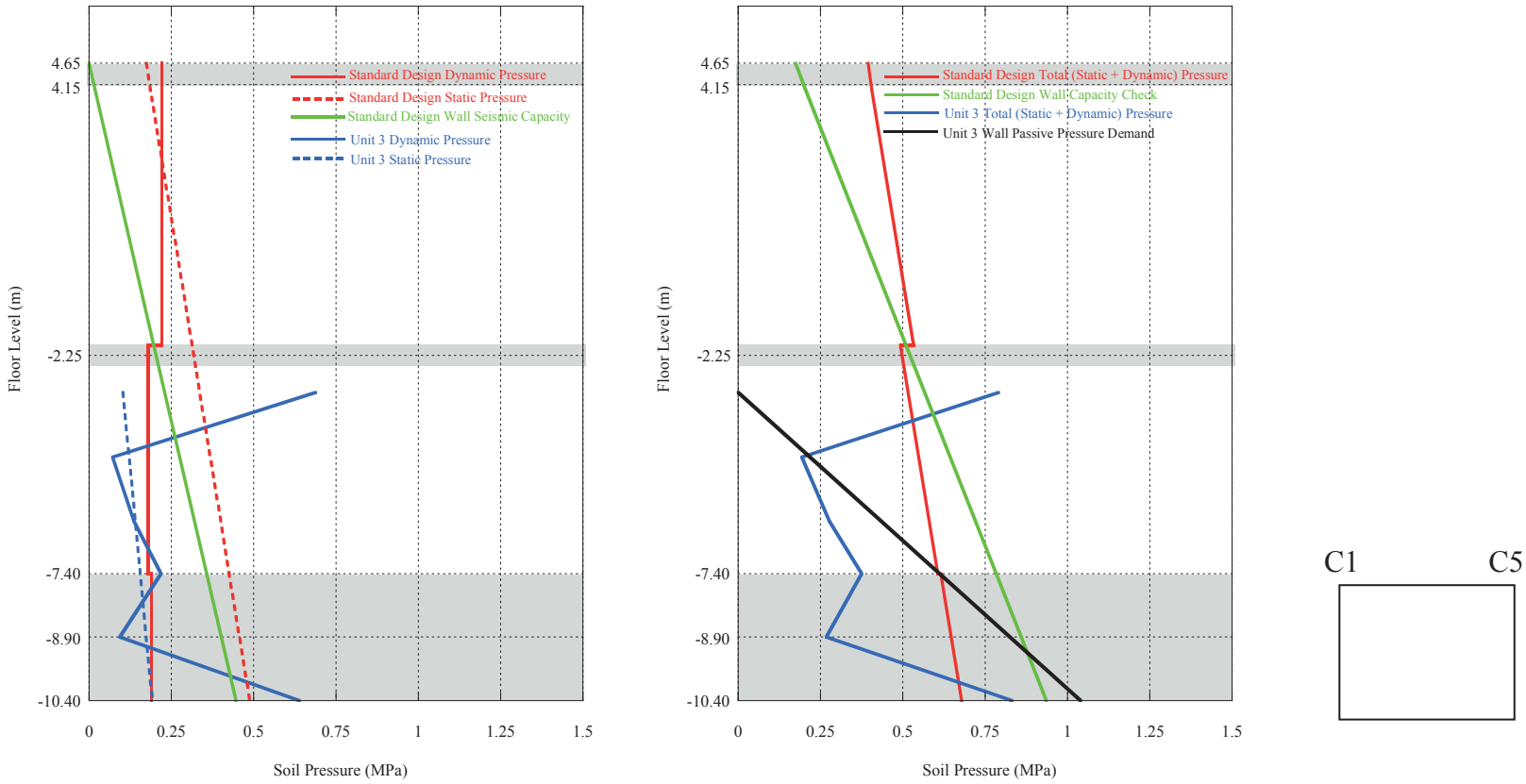

(a) Static Pressure and Dynamic Pressure **(b) Total Pressure and Wall Passive Pressure**

Note: The shaded area shows thickness of the floor slabs and basemat.

Figure 7-2: Lateral Pressure C5 Wall (Partial Column, SSE Envelope)

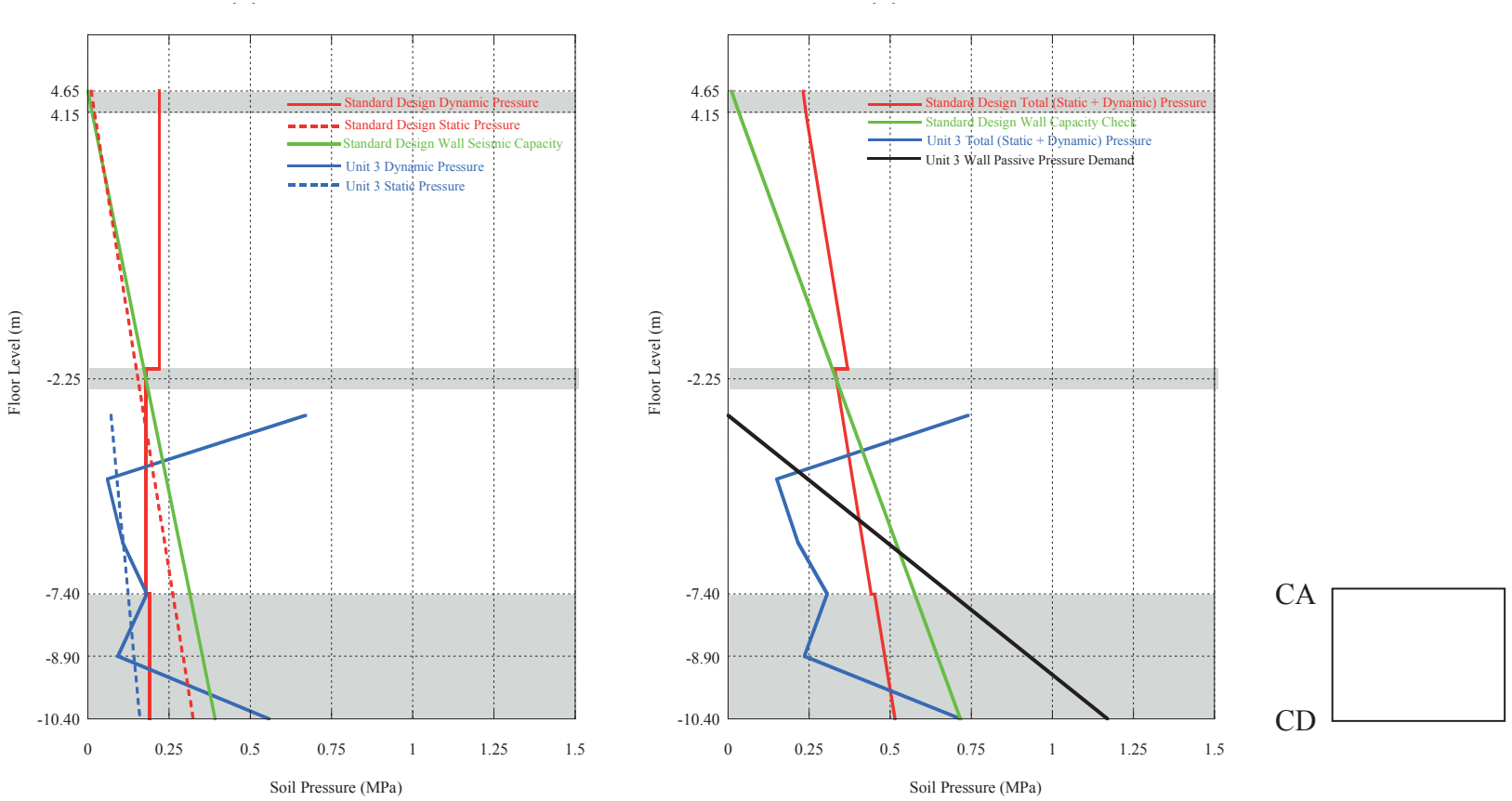

(a) Static Pressure and Dynamic Pressure **(b) Total Pressure and Wall Passive Pressure**

Note: The shaded area shows thickness of the floor slabs and basemat.

Figure 7-3: Lateral Pressure CA Wall (Partial Column, SSE Envelope)

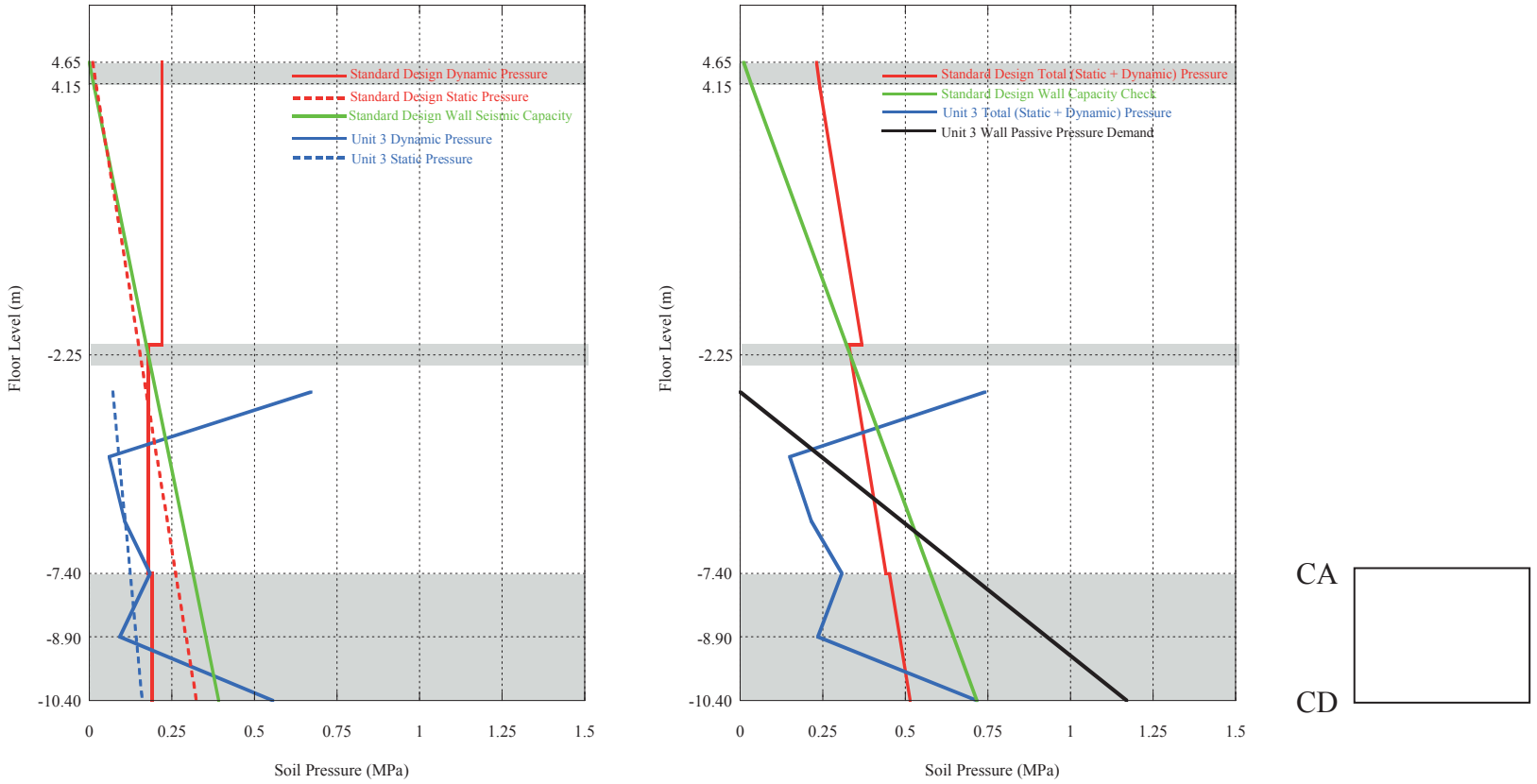

(a) Static Pressure and Dynamic Pressure **(b) Total Pressure and Wall Passive Pressure**

Note: The shaded area shows thickness of the floor slabs and basemat.

Figure 7-4: Lateral Pressure CD Wall (Partial Column, SSE Envelope)

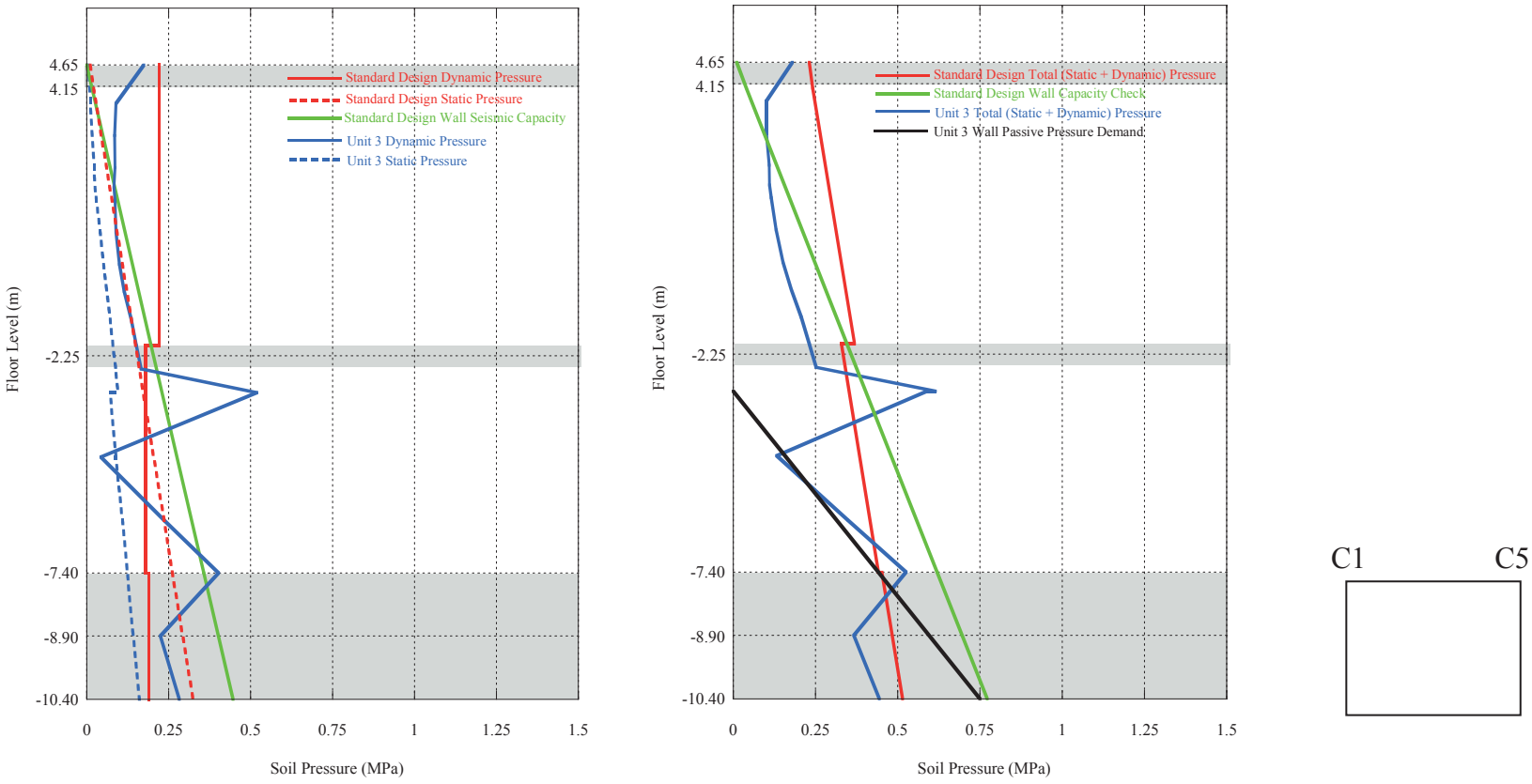

(a) Static Pressure and Dynamic Pressure **(b) Total Pressure and Wall Passive Pressure**

Note: The shaded area shows thickness of the floor slabs and basemat.

Figure 7-5: Lateral Pressure C1 Wall (Full Column, SSE Envelope)

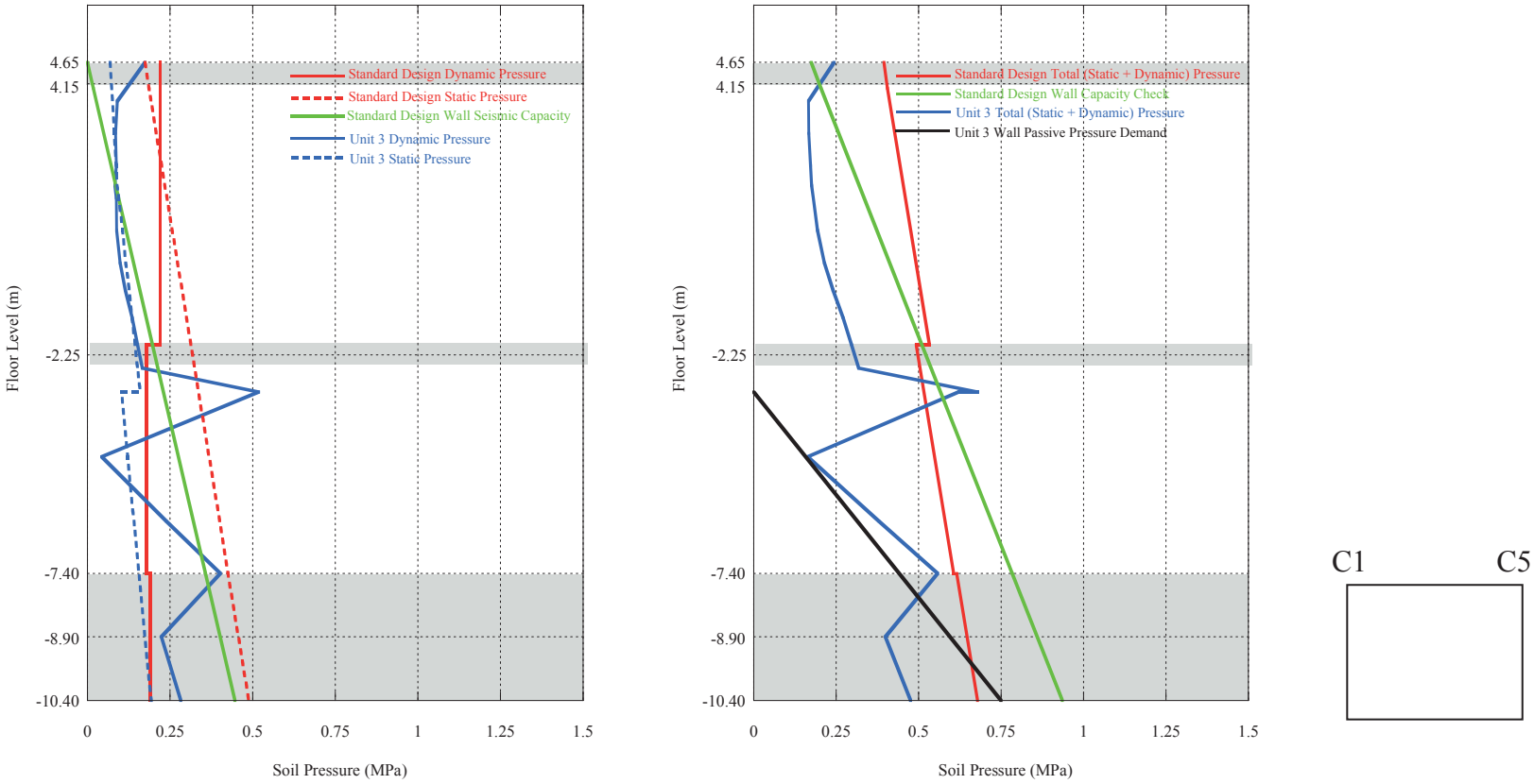

(a) Static Pressure and Dynamic Pressure **(b) Total Pressure and Wall Passive Pressure**

Note: The shaded area shows thickness of the floor slabs and basemat.

Figure 7-6: Lateral Pressure C5 Wall (Full Column, SSE Envelope)

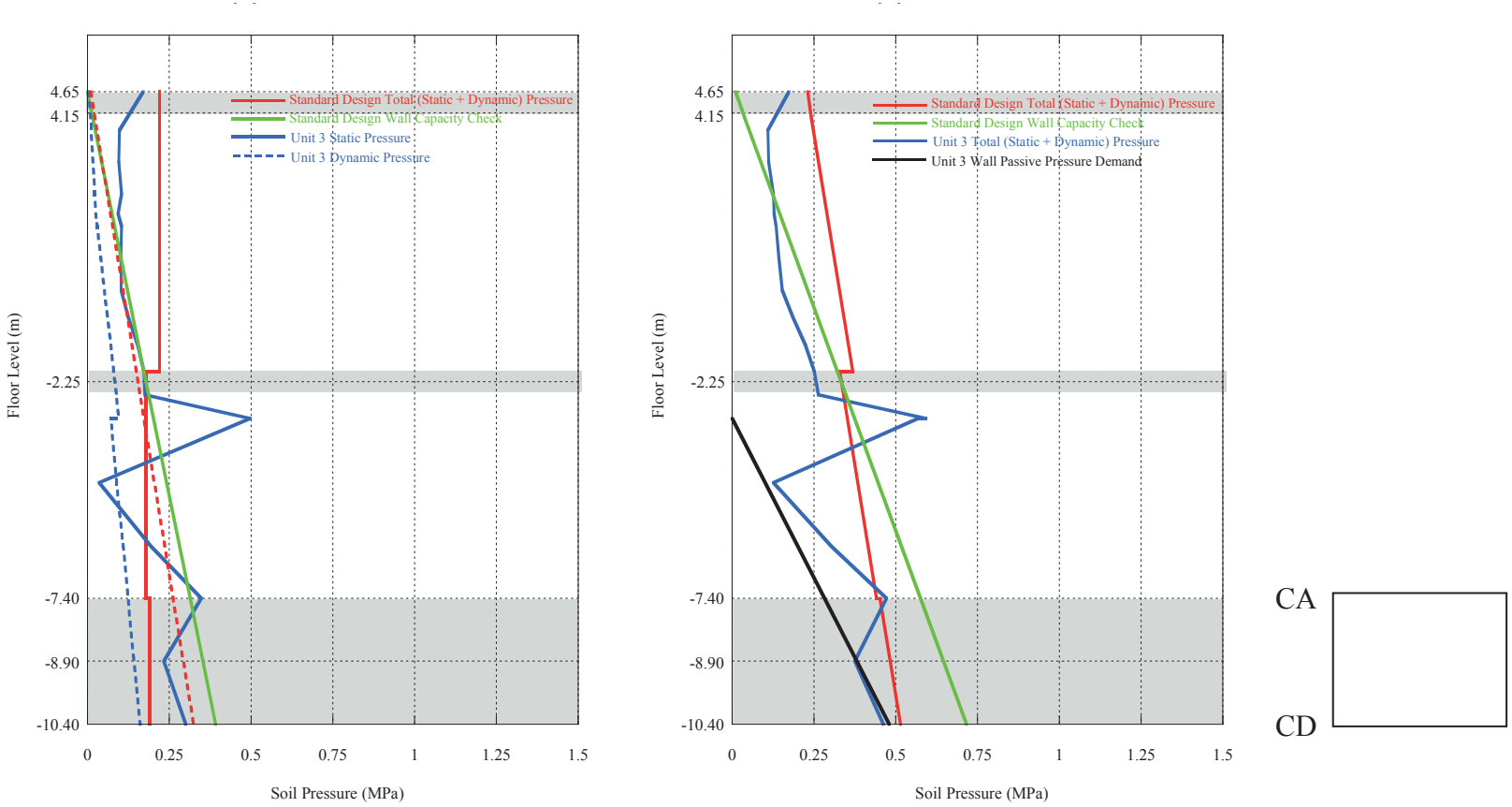

(a) Static Pressure and Dynamic Pressure **(b) Total Pressure and Wall Passive Pressure**

Note: The shaded area shows thickness of the floor slabs and basemat.

Figure 7-7: Lateral Pressure CA Wall (Full Column, SSE Envelope)

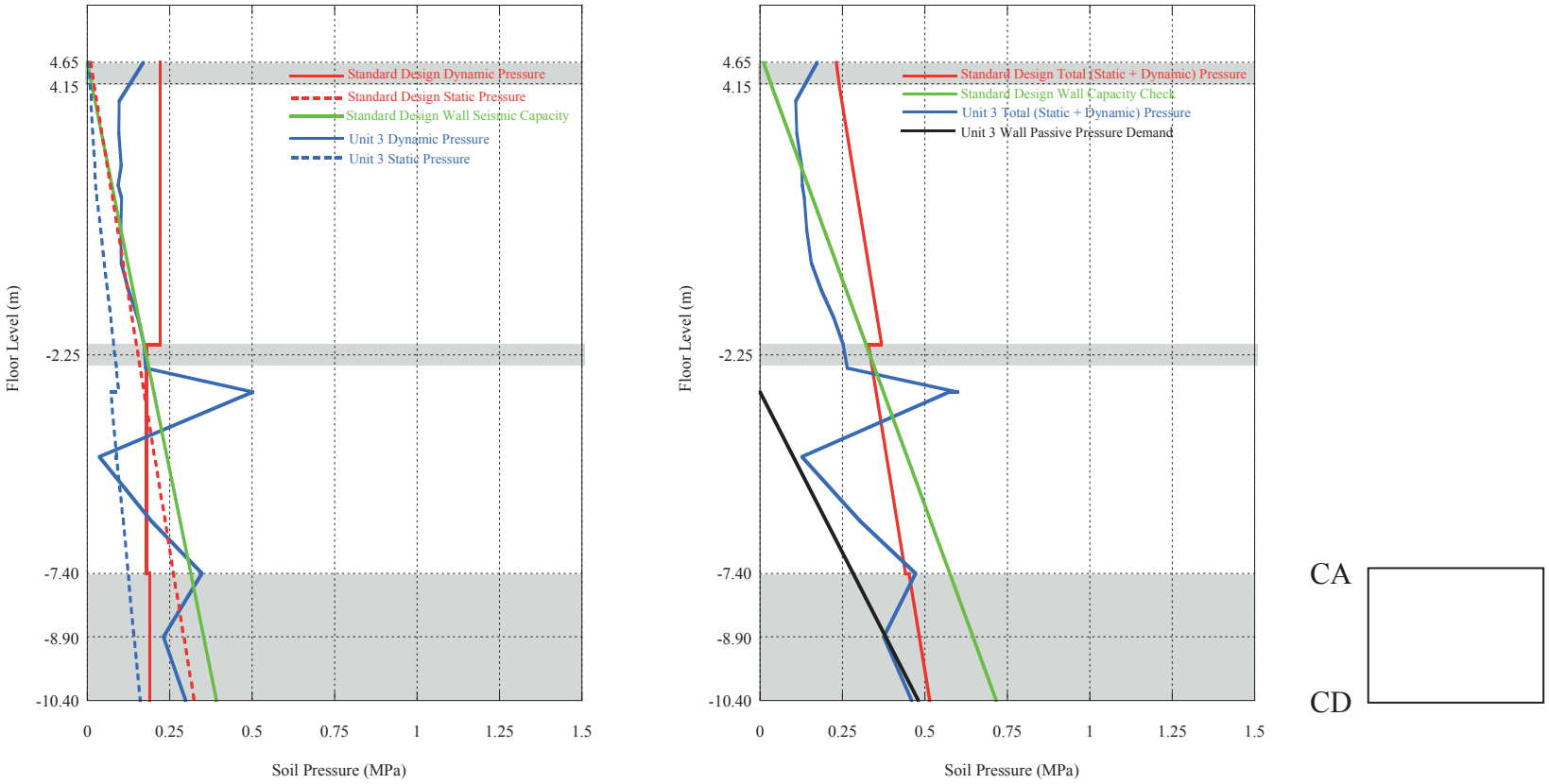

(a) Static Pressure and Dynamic Pressure **(b) Total Pressure and Wall Passive Pressure**

Note: The shaded area shows thickness of the floor slabs and basemat.

Figure 7-8: Lateral Pressure CD Wall (Full Column, SSE Envelope)

APPENDIX A
Evaluation of Overturning Stability

TABLE OF CONTENTS

LIST OF TABLES

A.1 SCOPE

This Appendix describes the detail of the evaluation of overturning stability for the CB.

A.2 EVALUATION OF THE KINETIC ENERGY OF EACH LUMPED MASS

The maximum velocities of the lumped masses, $(V_x)_i$, $(V_y)_i$ and $(V_z)_i$, relative to the ground described in Section 4, are obtained from the results of the SSI analyses provided in Reference 2-i for the maximum acceleration of each lumped mass using the following equations:

$$(V_x)_i = A_x \times T_{x1}/2\pi \ , \quad (V_y)_i = A_y \times T_{y1}/2\pi \ , \quad (V_z)_i = A_z \times T_{z1}/2\pi \quad \text{.....(A-1)}$$

where,

A_x, A_y, A_z = Maximum acceleration provided in Reference 2-i

T_{x1}, T_{y1}, T_{z1} = 1st natural vibration period of structure for Hard site provided in Reference 2-e

The peak horizontal and vertical ground velocities, $(V_H)_g$ and $(V_V)_g$, are the maximum values calculated by integrating the ground motion both in time and frequency domain. The acceleration Fourier spectra of the input time histories are translated to the velocity Fourier spectra. The maximum velocities are evaluated from the velocity time histories using inverse Fourier transformation

The calculated maximum velocity of the lumped masses, ground velocities, and calculated kinetic energy of each lumped mass are shown in Table A-1 through A-6.

A.3 EVALUATION OF DEAD WEIGHT AND BUOYANCY EFFECT

The calculated values to evaluate the effect of dead weight and buoyancy described in Figures 4-1 and 4-2 are shown in Table A-7.

Table A-1: Kinetic Energy of CB Lumped Masses for LB Partial Column Analysis Case 7

(a) NS Direction

Elevation (m)	Weight w (MN)	A_x (g)	$(V_x)_i$ (m/sec)	$(V_H)_g$ (m/sec)	$0.5m_iV_{Hi}^2$ (MN·m)
13.80	22	1.01	0.19	0.19	0.16
11.43	7	0.81	0.15	0.19	0.04
9.06	21	0.62	0.12	0.19	0.10
6.86	8	0.58	0.11	0.19	0.04
4.65	26	0.52	0.10	0.19	0.11
1.33	13	0.42	0.08	0.19	0.05
-2.00	25	0.49	0.09	0.19	0.10
-4.70	11	0.39	0.07	0.19	0.04
-7.40	36	0.37	0.07	0.19	0.12
-10.40	28	0.37	0.07	0.19	0.09
Total	197	-	-	-	0.85

(b) EW Direction

Elevation (m)	Weight w (MN)	A_y (g)	$(V_y)_i$ (m/sec)	$(V_H)_g$ (m/sec)	$0.5m_iV_{Hi}^2$ (MN·m)
13.80	22	0.89	0.18	0.16	0.13
11.43	7	0.77	0.16	0.16	0.04
9.06	21	0.72	0.15	0.16	0.10
6.86	8	0.70	0.14	0.16	0.04
4.65	26	0.65	0.13	0.16	0.11
1.33	13	0.46	0.09	0.16	0.04
-2.00	25	0.38	0.08	0.16	0.07
-4.70	11	0.30	0.06	0.16	0.03
-7.40	36	0.25	0.05	0.16	0.08
-10.40	28	0.26	0.05	0.16	0.06
Total	197	-	-	-	0.71

Table A-1: Kinetic Energy of CB Lumped Masses for LB Partial Column Analysis Case 7 (Continued)

(c) Z Direction

Elevation (m)	Weight w (MN)	A_z (g)	$(V_z)_i$ (m/sec)	$(V_v)_g$ (m/sec)	$0.5m_iV_{Vi}^2$ (MN·m)
13.80	22	0.72	0.08	0.15	0.06
11.43	7	0.71	0.08	0.15	0.02
9.06	21	0.68	0.07	0.15	0.06
6.86	8	0.65	0.07	0.15	0.02
4.65	26	0.63	0.07	0.15	0.06
1.33	13	0.57	0.06	0.15	0.03
-2.00	25	0.52	0.06	0.15	0.06
-4.70	11	0.48	0.05	0.15	0.02
-7.40	36	0.46	0.05	0.15	0.08
-10.40	28	0.46	0.05	0.15	0.06
Total	197	-	-	-	0.47

Table A-2: Kinetic Energy of CB Lumped Masses for BE Partial Column Analysis Case 8

(a) NS Direction

Elevation (m)	Weight w (MN)	A_x (g)	$(V_x)_i$ (m/sec)	$(V_H)_g$ (m/sec)	$0.5m_iV_{Hi}^2$ (MN·m)
13.80	22	1.24	0.23	0.19	0.20
11.43	7	1.07	0.20	0.19	0.06
9.06	21	0.90	0.17	0.19	0.14
6.86	8	0.78	0.15	0.19	0.05
4.65	26	0.73	0.14	0.19	0.14
1.33	13	0.56	0.11	0.19	0.06
-2.00	25	0.51	0.10	0.19	0.10
-4.70	11	0.41	0.08	0.19	0.04
-7.40	36	0.38	0.07	0.19	0.13
-10.40	28	0.38	0.07	0.19	0.10
Total	197	-	-	-	1.02

(b) EW Direction

Elevation (m)	Weight w (MN)	A_y (g)	$(V_y)_i$ (m/sec)	$(V_H)_g$ (m/sec)	$0.5m_iV_{Hi}^2$ (MN·m)
13.80	22	1.17	0.24	0.16	0.18
11.43	7	1.11	0.23	0.16	0.06
9.06	21	1.03	0.21	0.16	0.15
6.86	8	0.91	0.19	0.16	0.05
4.65	26	0.93	0.19	0.16	0.16
1.33	13	0.67	0.14	0.16	0.06
-2.00	25	0.52	0.11	0.16	0.09
-4.70	11	0.39	0.08	0.16	0.03
-7.40	36	0.39	0.08	0.16	0.11
-10.40	28	0.38	0.08	0.16	0.08
Total	197	-	-	-	0.96

Table A-2: Kinetic Energy of CB Lumped Masses for BE Partial Column Analysis Case 8 (Continued)

(c) Z Direction

Elevation (m)	Weight w (MN)	A_z (g)	$(V_z)_i$ (m/sec)	$(V_v)_g$ (m/sec)	$0.5m_iV_{Vi}^2$ (MN·m)
13.80	22	0.87	0.09	0.16	0.07
11.43	7	0.85	0.09	0.16	0.02
9.06	21	0.82	0.09	0.16	0.07
6.86	8	0.78	0.09	0.16	0.02
4.65	26	0.73	0.08	0.16	0.07
1.33	13	0.64	0.07	0.16	0.03
-2.00	25	0.55	0.06	0.16	0.06
-4.70	11	0.51	0.06	0.16	0.02
-7.40	36	0.54	0.06	0.16	0.08
-10.40	28	0.53	0.06	0.16	0.07
Total	197	-	-	-	0.52

Table A-3: Kinetic Energy of CB Lumped Masses for UB Partial Column Analysis Case 9

(a) NS Direction

Elevation (m)	Weight w (MN)	A_x (g)	$(V_x)_i$ (m/sec)	$(V_H)_g$ (m/sec)	$0.5m_iV_{Hi}^2$ (MN·m)
13.80	22	1.63	0.30	0.19	0.27
11.43	7	1.45	0.27	0.19	0.08
9.06	21	1.26	0.24	0.19	0.20
6.86	8	1.05	0.20	0.19	0.06
4.65	26	0.88	0.16	0.19	0.17
1.33	13	0.65	0.12	0.19	0.07
-2.00	25	0.63	0.12	0.19	0.12
-4.70	11	0.45	0.08	0.19	0.04
-7.40	36	0.48	0.09	0.19	0.15
-10.40	28	0.48	0.09	0.19	0.11
Total	197	-	-	-	1.28

(b) EW Direction

Elevation (m)	Weight w (MN)	A_y (g)	$(V_y)_i$ (m/sec)	$(V_H)_g$ (m/sec)	$0.5m_iV_{Hi}^2$ (MN·m)
13.80	22	1.55	0.31	0.16	0.25
11.43	7	1.32	0.27	0.16	0.07
9.06	21	1.12	0.23	0.16	0.17
6.86	8	1.07	0.22	0.16	0.06
4.65	26	0.98	0.20	0.16	0.17
1.33	13	0.74	0.15	0.16	0.07
-2.00	25	0.67	0.13	0.16	0.11
-4.70	11	0.50	0.10	0.16	0.04
-7.40	36	0.43	0.09	0.16	0.12
-10.40	28	0.43	0.09	0.16	0.09
Total	197	-	-	-	1.14

Table A-3: Evaluation of Kinetic Energy at the Lumped Masses for UB Partial Column Analysis Case 9 (Continued)

(c) Z Direction

Elevation (m)	Weight w (MN)	A_z (g)	$(V_z)_i$ (m/sec)	$(V_v)_g$ (m/sec)	$0.5m_iV_{Vi}^2$ (MN·m)
13.80	22	1.05	0.11	0.16	0.08
11.43	7	1.01	0.11	0.16	0.03
9.06	21	0.95	0.10	0.16	0.07
6.86	8	0.88	0.10	0.16	0.03
4.65	26	0.82	0.09	0.16	0.08
1.33	13	0.70	0.08	0.16	0.04
-2.00	25	0.60	0.07	0.16	0.06
-4.70	11	0.62	0.07	0.16	0.03
-7.40	36	0.64	0.07	0.16	0.09
-10.40	28	0.63	0.07	0.16	0.07
Total	197	-	-	-	0.58

Table A-4: Kinetic Energy of CB Lumped Masses for LB Full Column Analysis Case 10

(a) NS Direction

Elevation (m)	Weight w (MN)	A_x (g)	$(V_x)_i$ (m/sec)	$(V_H)_g$ (m/sec)	$0.5m_iV_{Hi}^2$ (MN·m)
13.80	22	0.84	0.16	0.18	0.13
11.43	7	0.74	0.14	0.18	0.04
9.06	21	0.63	0.12	0.18	0.10
6.86	8	0.52	0.10	0.18	0.03
4.65	26	0.42	0.08	0.18	0.09
1.33	13	0.34	0.06	0.18	0.04
-2.00	25	0.33	0.06	0.18	0.07
-4.70	11	0.29	0.05	0.18	0.03
-7.40	36	0.27	0.05	0.18	0.10
-10.40	28	0.28	0.05	0.18	0.08
Total	197	-	-	-	0.70

(b) EW Direction

Elevation (m)	Weight w (MN)	A_y (g)	$(V_y)_i$ (m/sec)	$(V_H)_g$ (m/sec)	$0.5m_iV_{Hi}^2$ (MN·m)
13.80	22	0.80	0.16	0.16	0.12
11.43	7	0.68	0.14	0.16	0.03
9.06	21	0.57	0.12	0.16	0.09
6.86	8	0.51	0.10	0.16	0.03
4.65	26	0.45	0.09	0.16	0.08
1.33	13	0.33	0.07	0.16	0.04
-2.00	25	0.32	0.07	0.16	0.07
-4.70	11	0.30	0.06	0.16	0.03
-7.40	36	0.29	0.06	0.16	0.09
-10.40	28	0.30	0.06	0.16	0.07
Total	197	-	-	-	0.64

Table A-4: Kinetic Energy of CB Lumped Masses for LB Full Column Analysis Case 10 (Continued)

(c) Z Direction

Elevation (m)	Weight w (MN)	A_z (g)	$(V_z)_i$ (m/sec)	$(V_v)_g$ (m/sec)	$0.5m_iV_{Vi}^2$ (MN·m)
13.80	22	0.60	0.07	0.17	0.06
11.43	7	0.59	0.06	0.17	0.02
9.06	21	0.57	0.06	0.17	0.06
6.86	8	0.55	0.06	0.17	0.02
4.65	26	0.52	0.06	0.17	0.07
1.33	13	0.46	0.05	0.17	0.03
-2.00	25	0.41	0.04	0.17	0.06
-4.70	11	0.38	0.04	0.17	0.03
-7.40	36	0.36	0.04	0.17	0.08
-10.40	28	0.36	0.04	0.17	0.06
Total	197	-	-	-	0.51

Table A-5: Kinetic Energy of CB Lumped Masses for BE Full Column Analysis Case 11

(a) NS Direction

Elevation (m)	Weight w (MN)	A_x (g)	$(V_x)_i$ (m/sec)	$(V_H)_g$ (m/sec)	$0.5m_iV_{Hi}^2$ (MN·m)
13.80	22	0.85	0.16	0.19	0.13
11.43	7	0.75	0.14	0.19	0.04
9.06	21	0.66	0.12	0.19	0.11
6.86	8	0.57	0.11	0.19	0.04
4.65	26	0.50	0.09	0.19	0.10
1.33	13	0.36	0.07	0.19	0.04
-2.00	25	0.40	0.07	0.19	0.09
-4.70	11	0.31	0.06	0.19	0.03
-7.40	36	0.31	0.06	0.19	0.11
-10.40	28	0.31	0.06	0.19	0.09
Total	197	-	-	-	0.78

(b) EW Direction

Elevation (m)	Weight w (MN)	A_y (g)	$(V_y)_i$ (m/sec)	$(V_H)_g$ (m/sec)	$0.5m_iV_{Hi}^2$ (MN·m)
13.80	22	0.87	0.18	0.15	0.12
11.43	7	0.67	0.14	0.15	0.03
9.06	21	0.63	0.13	0.15	0.09
6.86	8	0.59	0.12	0.15	0.03
4.65	26	0.53	0.11	0.15	0.09
1.33	13	0.35	0.07	0.15	0.03
-2.00	25	0.35	0.07	0.15	0.06
-4.70	11	0.30	0.06	0.15	0.03
-7.40	36	0.33	0.07	0.15	0.09
-10.40	28	0.33	0.07	0.15	0.07
Total	197	-	-	-	0.64

Table A-5: Kinetic Energy of CB Lumped Masses (for BE Full Column Analysis Case 11 (Continued)

(c) Z Direction

Elevation (m)	Weight w (MN)	A_z (g)	$(V_z)_i$ (m/sec)	$(V_v)_g$ (m/sec)	$0.5m_iV_{Vi}^2$ (MN·m)
13.80	22	0.65	0.07	0.18	0.07
11.43	7	0.63	0.07	0.18	0.02
9.06	21	0.61	0.07	0.18	0.06
6.86	8	0.58	0.06	0.18	0.02
4.65	26	0.56	0.06	0.18	0.07
1.33	13	0.51	0.06	0.18	0.04
-2.00	25	0.45	0.05	0.18	0.06
-4.70	11	0.41	0.04	0.18	0.03
-7.40	36	0.39	0.04	0.18	0.09
-10.40	28	0.39	0.04	0.18	0.07
Total	197	-	-	-	0.54

Table A-6: Kinetic Energy of CB Lumped Masses for UB Full Column Analysis Case 12

(a) NS Direction

Elevation (m)	Weight w (MN)	A_x (g)	$(V_x)_i$ (m/sec)	$(V_H)_g$ (m/sec)	$0.5m_iV_{Hi}^2$ (MN·m)
13.80	22	1.07	0.20	0.19	0.17
11.43	7	0.87	0.16	0.19	0.05
9.06	21	0.74	0.14	0.19	0.12
6.86	8	0.68	0.13	0.19	0.04
4.65	26	0.62	0.12	0.19	0.13
1.33	13	0.51	0.10	0.19	0.06
-2.00	25	0.49	0.09	0.19	0.10
-4.70	11	0.35	0.07	0.19	0.04
-7.40	36	0.33	0.06	0.19	0.12
-10.40	28	0.33	0.06	0.19	0.09
Total	197	-	-	-	0.92

(b) EW Direction

Elevation (m)	Weight w (MN)	A_y (g)	$(V_y)_i$ (m/sec)	$(V_H)_g$ (m/sec)	$0.5m_iV_{Hi}^2$ (MN·m)
13.80	22	0.93	0.19	0.16	0.14
11.43	7	0.78	0.16	0.16	0.04
9.06	21	0.72	0.15	0.16	0.10
6.86	8	0.64	0.13	0.16	0.04
4.65	26	0.53	0.11	0.16	0.10
1.33	13	0.42	0.08	0.16	0.04
-2.00	25	0.43	0.09	0.16	0.08
-4.70	11	0.35	0.07	0.16	0.03
-7.40	36	0.32	0.07	0.16	0.10
-10.40	28	0.32	0.06	0.16	0.07
Total	197	-	-	-	0.73

Table A-6: Evaluation of Kinetic Energy at the Lumped Masses for UB Full Column Analysis Case 12 (Continued)

(c) Z Direction

Elevation (m)	Weight w (MN)	A_z (g)	$(V_z)_i$ (m/sec)	$(V_v)_g$ (m/sec)	$0.5m_iV_{Vi}^2$ (MN·m)
13.80	22	0.81	0.09	0.18	0.08
11.43	7	0.79	0.09	0.18	0.03
9.06	21	0.76	0.08	0.18	0.07
6.86	8	0.72	0.08	0.18	0.03
4.65	26	0.66	0.07	0.18	0.08
1.33	13	0.58	0.06	0.18	0.04
-2.00	25	0.58	0.06	0.18	0.07
-4.70	11	0.56	0.06	0.18	0.03
-7.40	36	0.54	0.06	0.18	0.10
-10.40	28	0.54	0.06	0.18	0.08
Total	197	-	-	-	0.62

Table A-7: Calculation of Gravity Force and Buoyancy Effect

Direction		NS	EW
Dead Weight Effect			
Dead Weight	; m_0g(MN)	197	197
The Height of Mass Center;			
at the stable position	; h_s (m)	10.95	10.95
at the overturning position	; h_o (m)	18.69	16.17
$h=h_o-h_s$	; h (m)	7.74	5.22
Potential Energy Needed to Lift the Structure to the Overturning Position;	; m_0gh (MN·m)	1525	1028
Buoyancy Force Effect			
Rotation of Basemat at the Overturning Position;	; Θ (deg)	54.14	47.38
Water Depth;	; d (m)	12.16	12.16
The Center of Buoyancy;			
at the Stable Position	; H_{sp} (m)	6.08	6.08
at the Overturning Position	; H_{op} (m)	8.10	8.10
Buoyancy;			
at the Stable Position	; V_{sp} (MN)	86	86
at the Overturning Position	; V_{op} (MN)	36	44
Potential Energy Caused by the Effect of Buoyancy	; W_b (MN·m)	123.9	131.7

APPENDIX B
SASSI2010 Base Reaction Time Histories

LIST OF FIGURES

B.1 SCOPE

Appendix B presents the time histories for the sliding evaluation and bearing pressure evaluation of the CB with full (uncracked concrete) stiffness properties for the LB, BE, and UB partial and full column soil profiles.

All of the time histories shown in Appendix B are obtained by the algebraic sum of the spring force in three components of input motion in the time domain as described in Section 5.6 of Reference 2-i. The static gravity and buoyancy forces are added to the vertical seismic base reaction time histories as shown Equation 5-2.

As explained in Sections 5 and 6, the evaluations of the sliding stability and dynamic bearing pressures are performed for each step of the time histories. The plots in Figures B-1 (a through l) identify the critical time when the maximum lateral pressure demands on the subgrade are calculated. The plots in Figures B-1 (a through l) identify the critical time when the maximum lateral pressure demands on the subgrade are calculated. The instances when the maximum dynamic bearing pressures are calculated are identified in the plots in Figures B-2 (a through l).

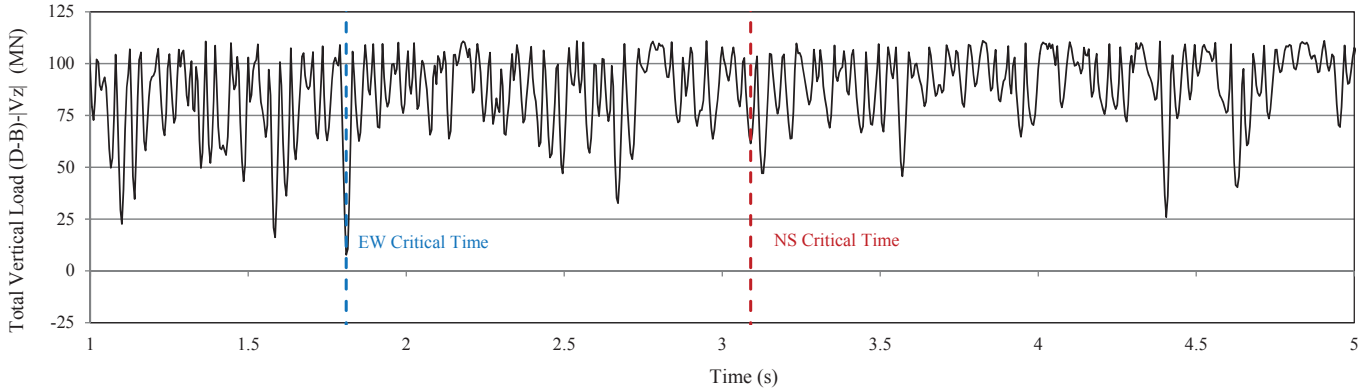

(a) Total Vertical Load

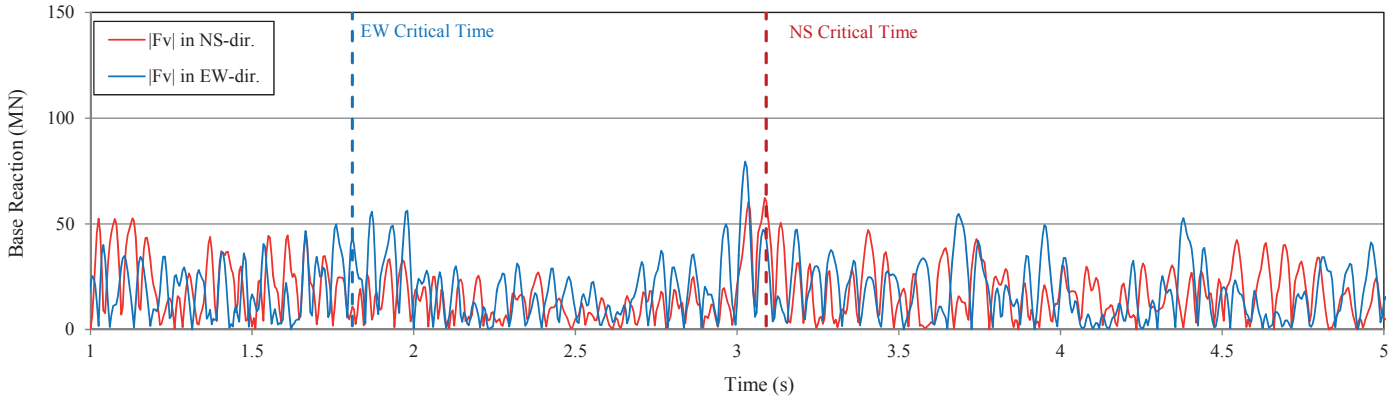

(b) Horizontal Driving Seismic Force

Figure B-1a: CB Sliding Evaluation - Basemat Bottom Reactions Time Histories from LB Partial Column Profile Analysis Case 7

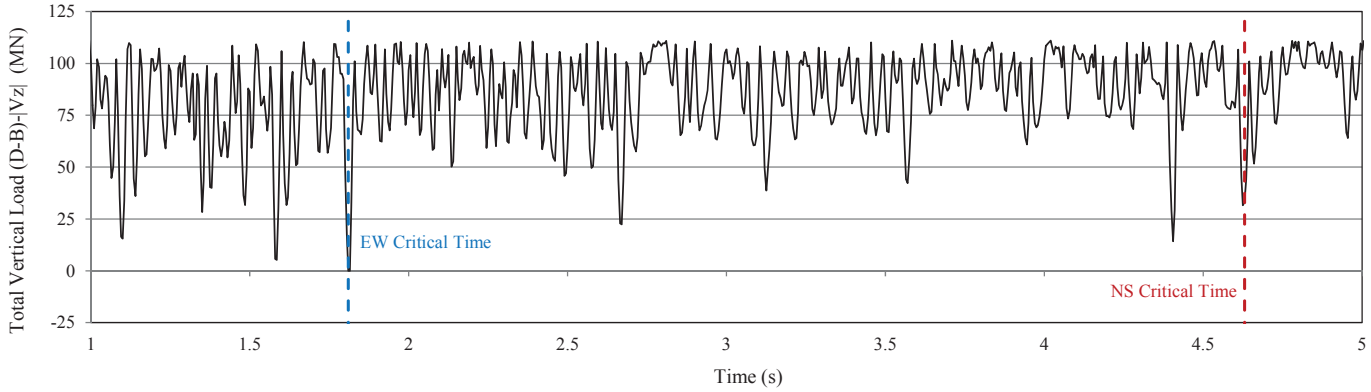

(a) Total Vertical Load

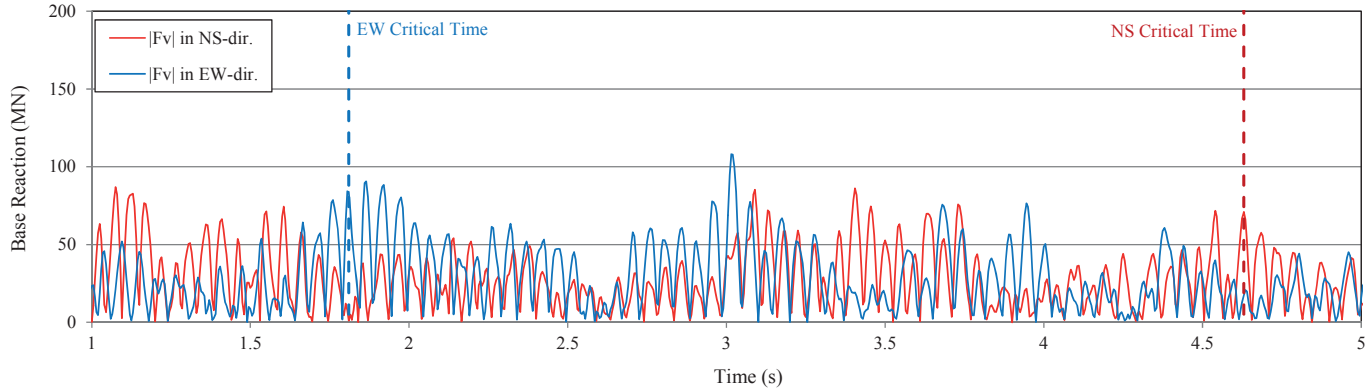

(b) Horizontal Driving Seismic Force

Figure B-1b: CB Sliding Evaluation - Basemat Bottom Reactions Time Histories from BE Partial Column Profile Analysis Case 8

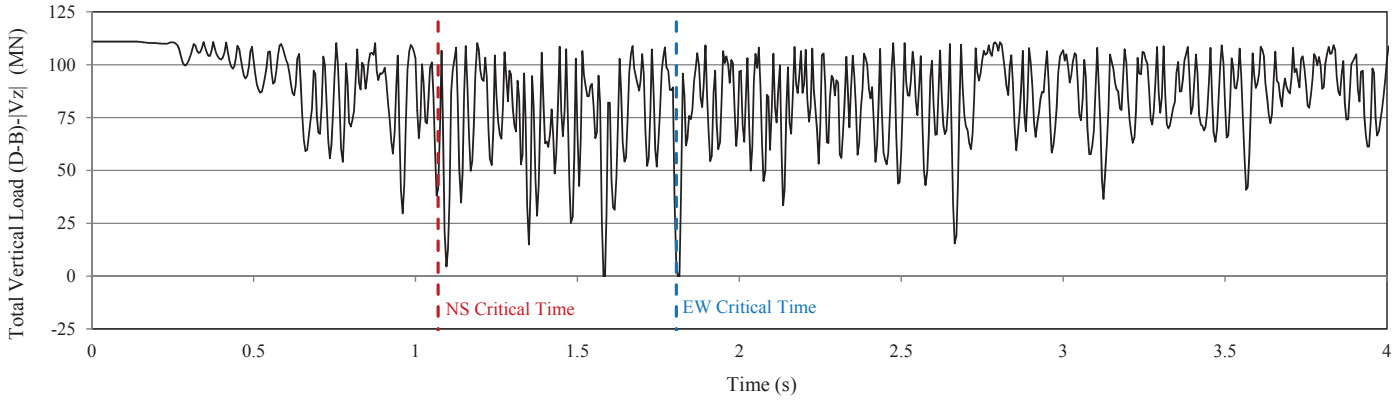

(a) Total Vertical Load

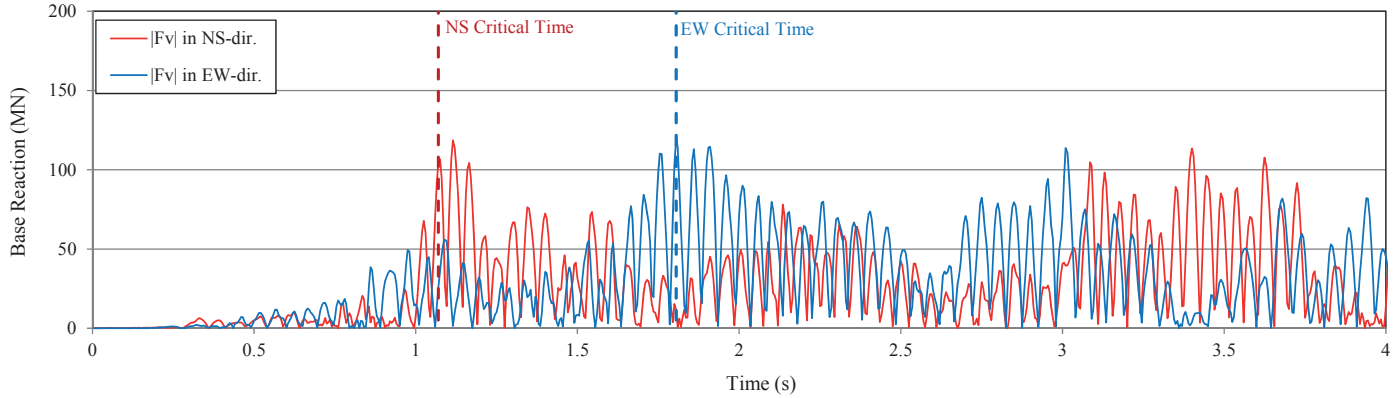

(b) Horizontal Driving Seismic Force

Figure B-1c: CB Sliding Evaluation - Basemat Bottom Reactions Time Histories from UB Partial Column Profile Analysis Case 9

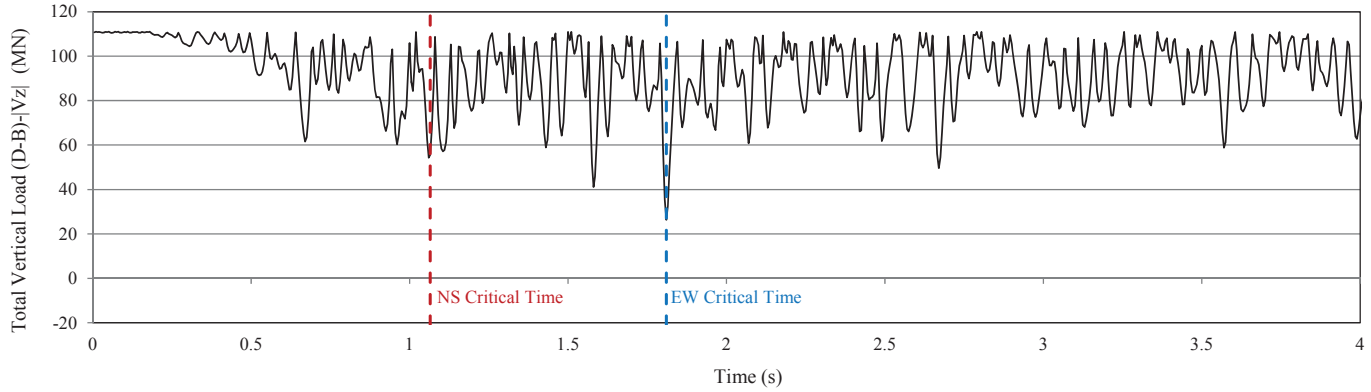

(a) Total Vertical Load

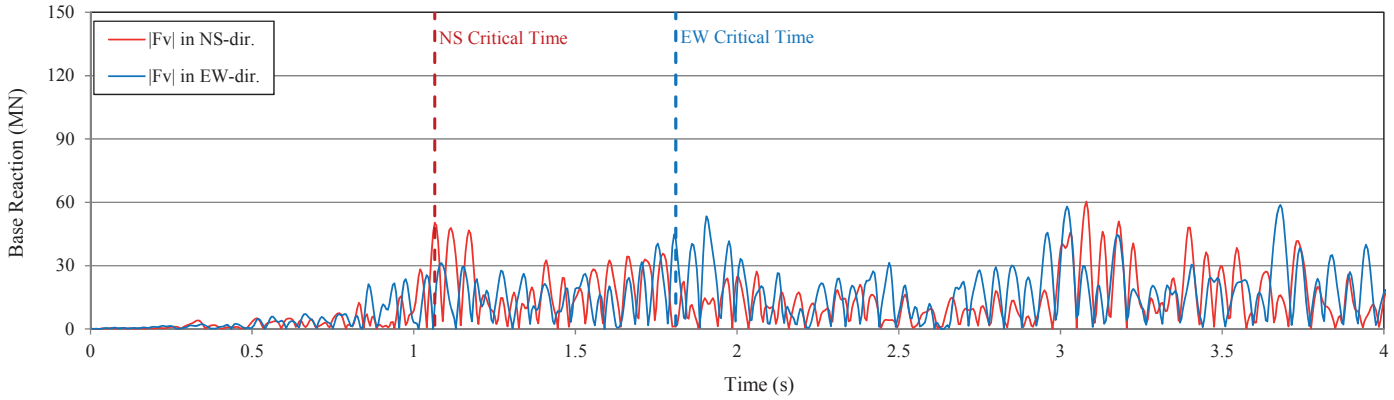

(b) Horizontal Driving Seismic Force

Figure B-1d: CB Sliding Evaluation - Basemat Bottom Reactions Time Histories from LB Full Column Profile Analysis Case 10

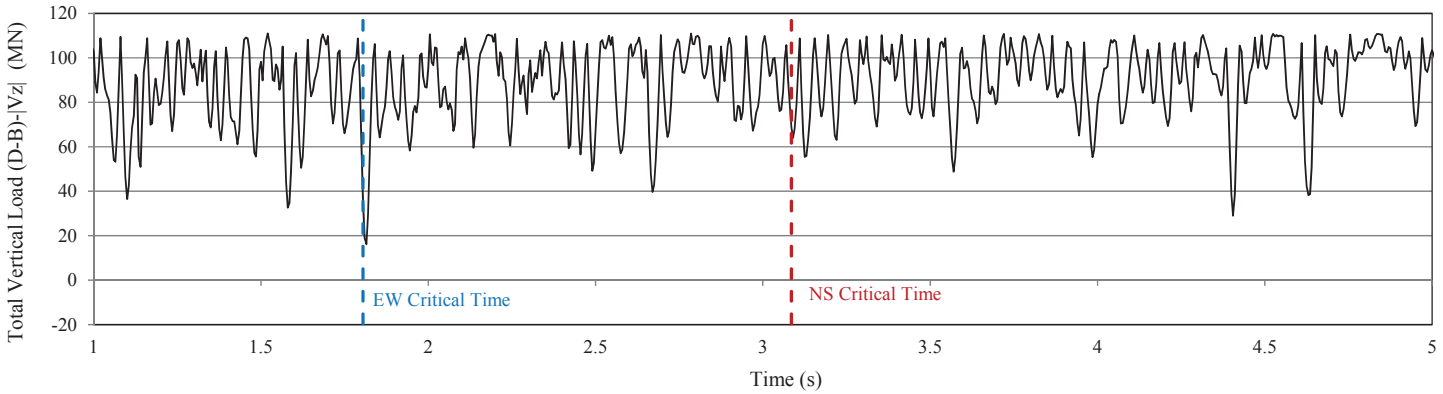

(a) Total Vertical Load

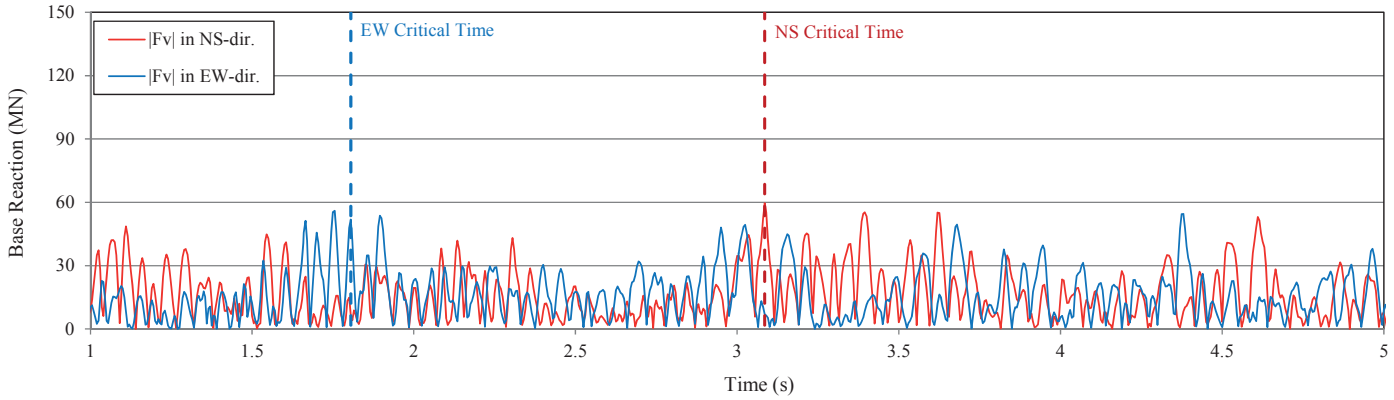

(b) Horizontal Driving Seismic Force

Figure B-1e: CB Sliding Evaluation - Basemat Bottom Reactions Time Histories from BE Full Column Profile Analysis Case 11

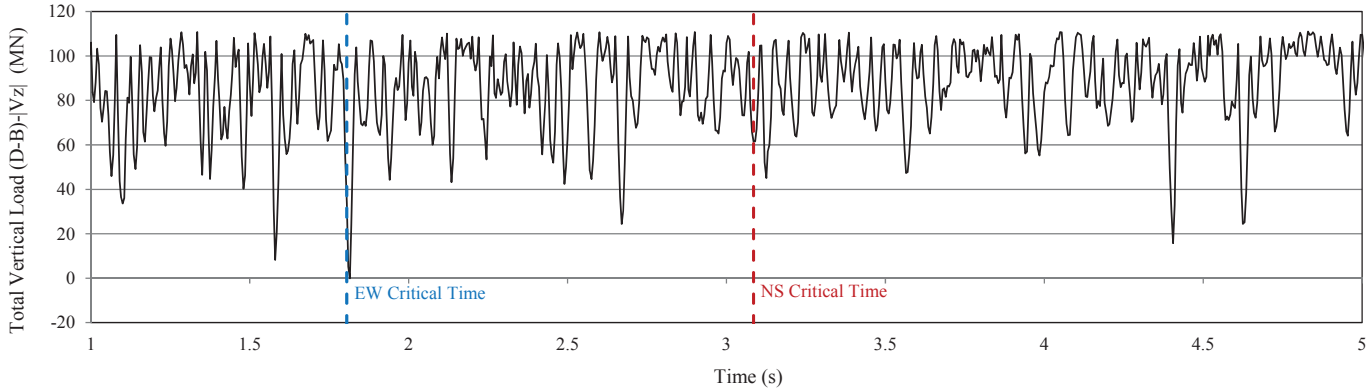

(a) Total Vertical Load

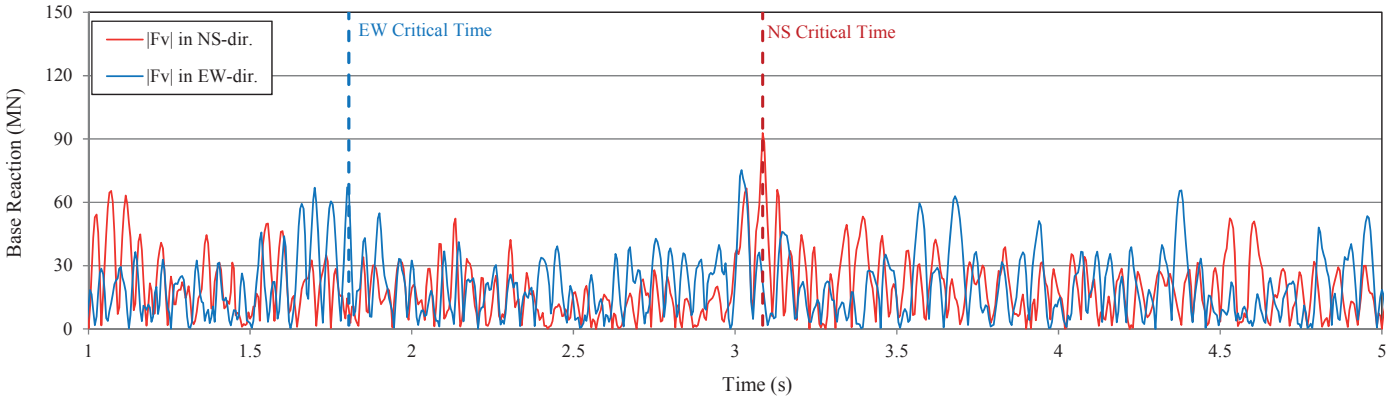

(b) Horizontal Driving Seismic Force

Figure B-1f: CB Sliding Evaluation - Basemat Bottom Reactions Time Histories from UB Full Column Profile Analysis Case 12

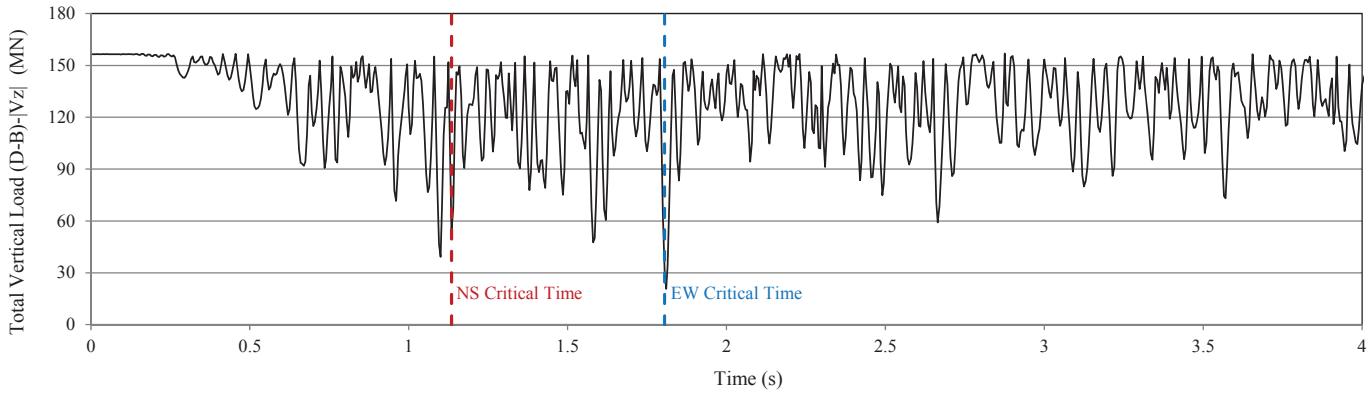

(a) Total Vertical Load

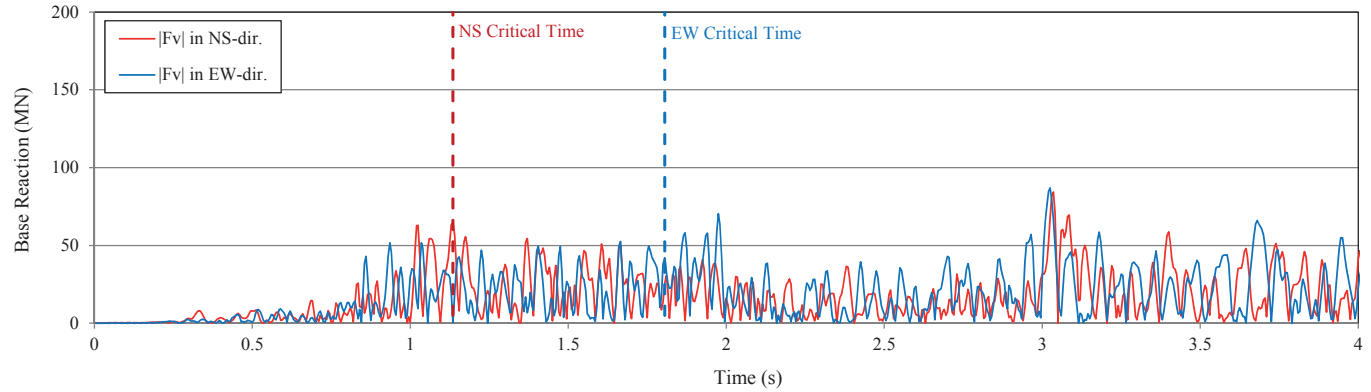

(b) Horizontal Driving Seismic Force

Figure B-1g: CB Sliding Evaluation – Concrete Fill Bottom Reactions Time Histories from LB Partial Column Profile Analysis Case 7

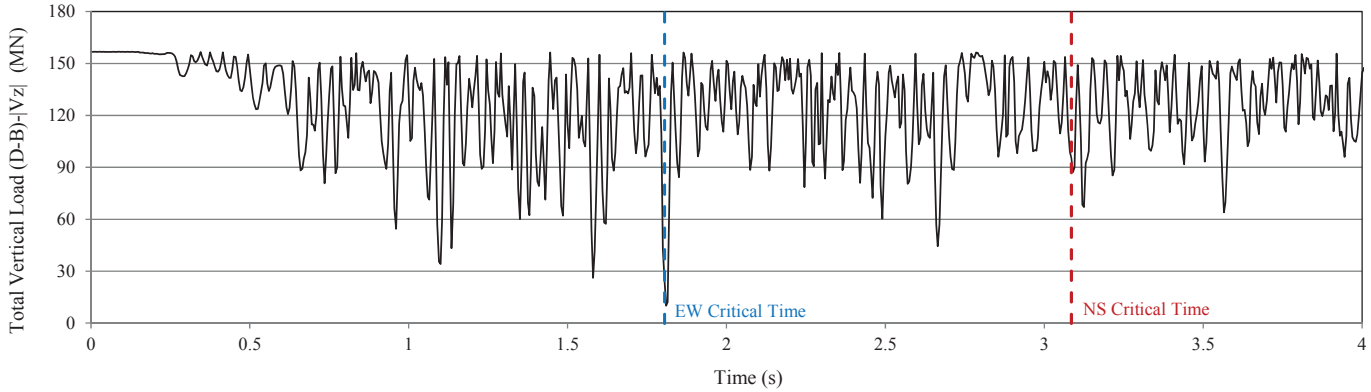

(a) Total Vertical Load

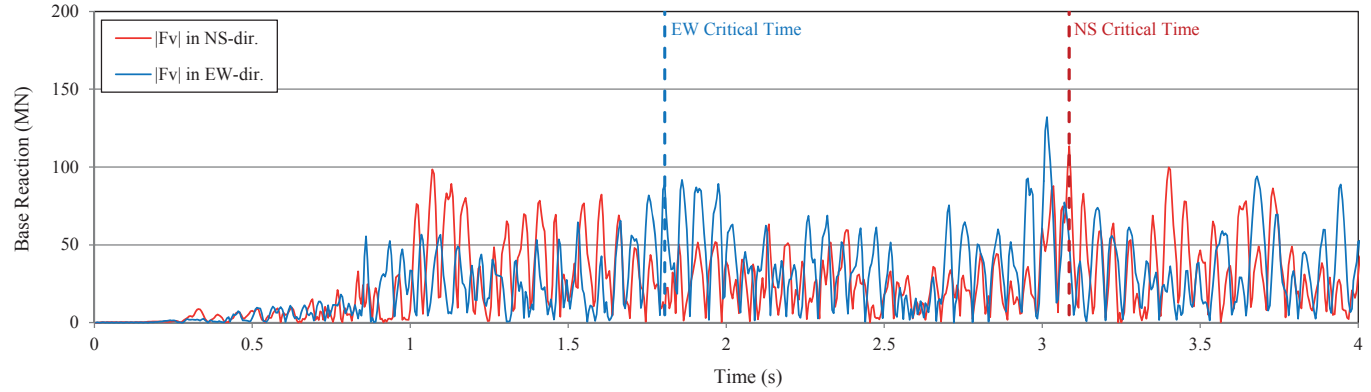

(b) Horizontal Driving Seismic Force

Figure B-1h: CB Sliding Evaluation - Concrete Fill Bottom Reactions Time Histories from BE Partial Column Profile Analysis Case 8

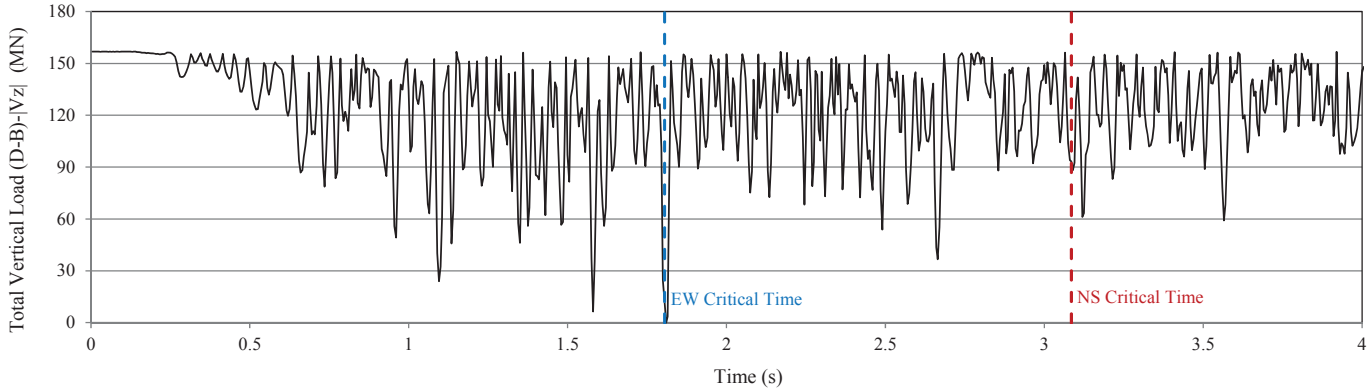

(a) Total Vertical Load

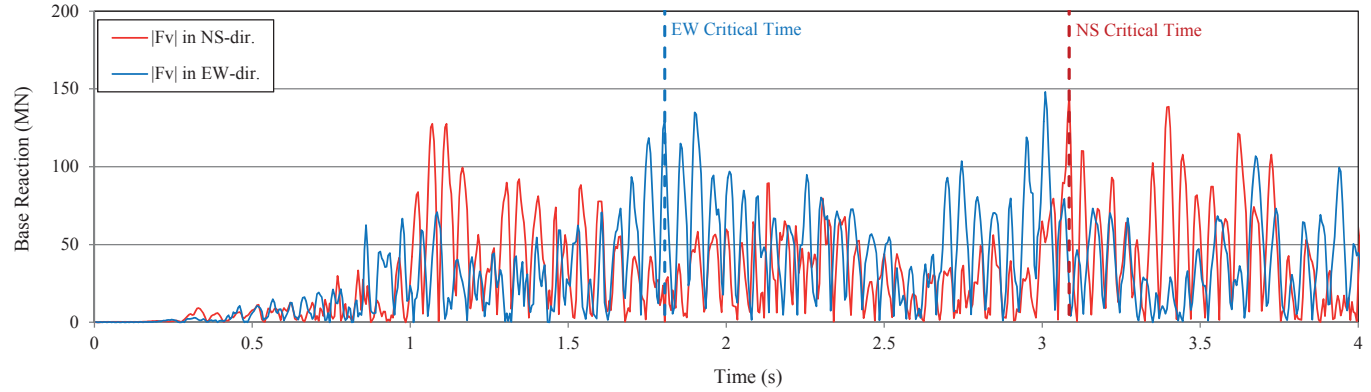

(b) Horizontal Driving Seismic Force

Figure B-1i: CB Sliding Evaluation - Concrete Fill Bottom Reactions Time Histories from UB Partial Column Profile Analysis Case 9

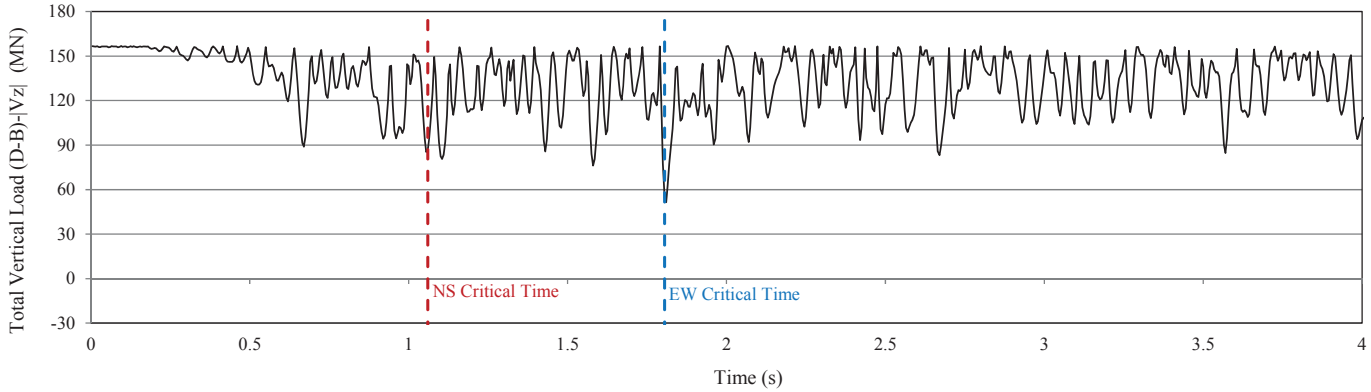

(a) Total Vertical Load

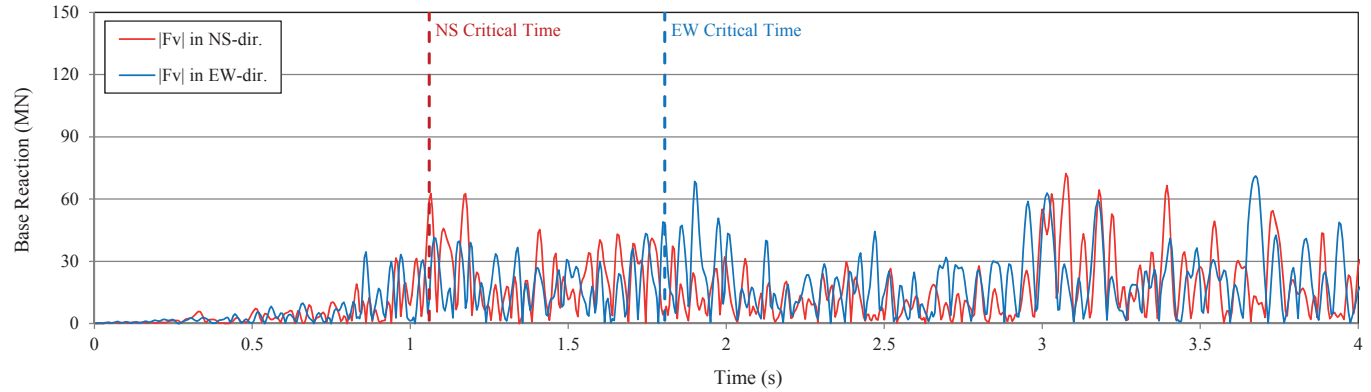

(b) Horizontal Driving Seismic Force

Figure B-1j: CB Sliding Evaluation - Concrete Fill Bottom Reactions Time Histories from LB Full Column Profile Analysis Case 10

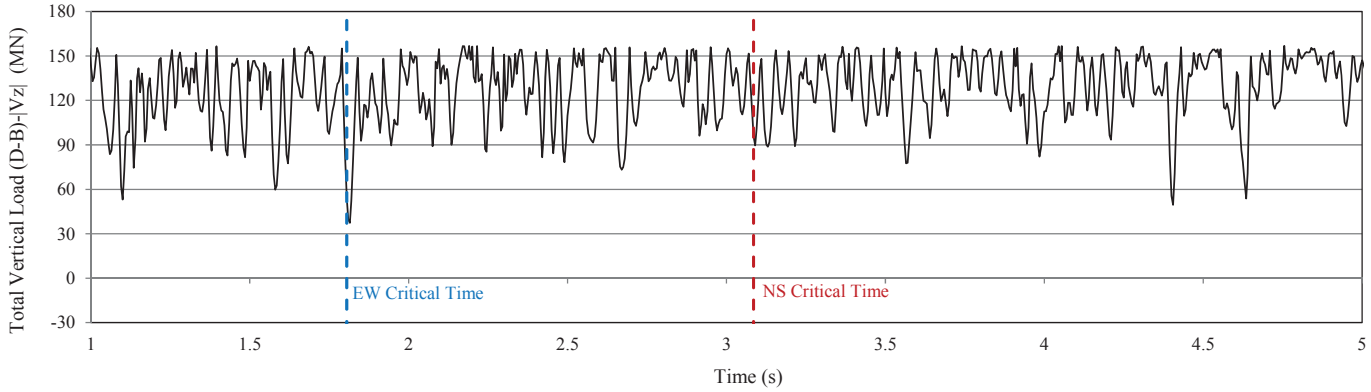

(a) Total Vertical Load

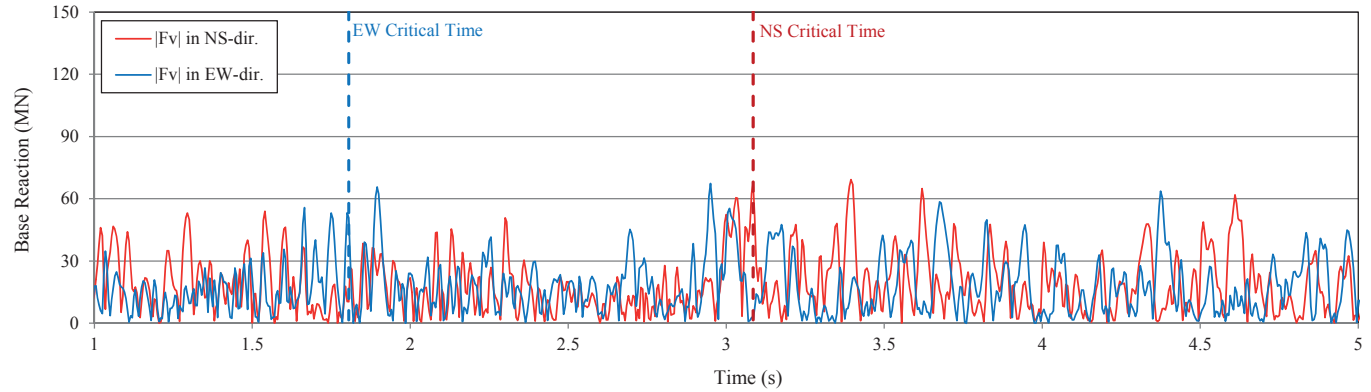

(b) Horizontal Driving Seismic Force

Figure B-1k: CB Sliding Evaluation - Concrete Fill Bottom Reactions Time Histories from BE Full Column Profile Analysis Case 11

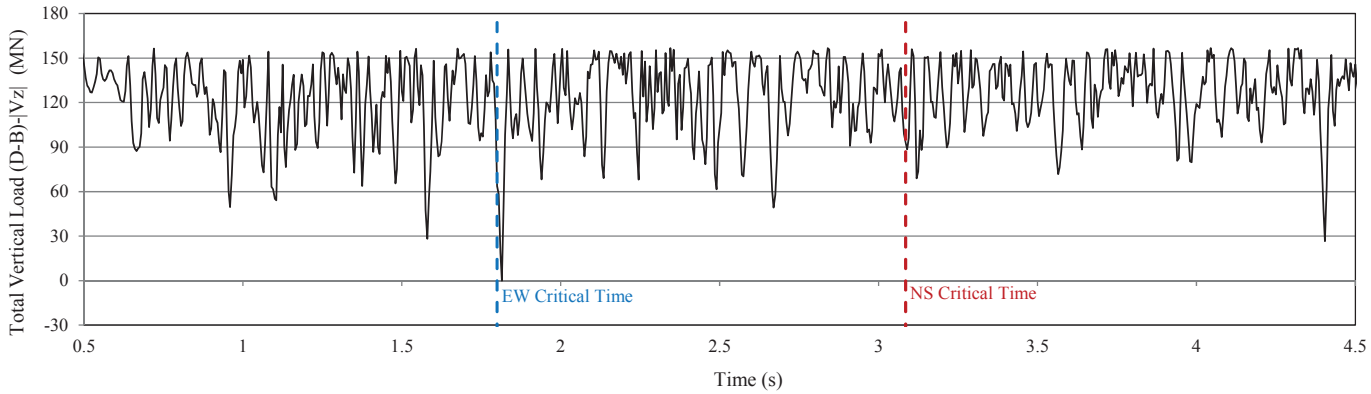

(a) Total Vertical Load

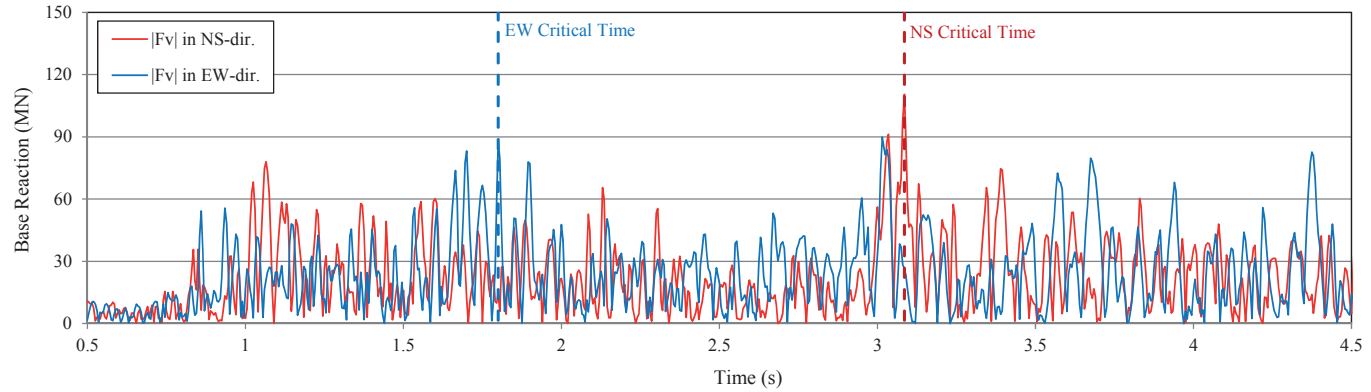

(b) Horizontal Driving Seismic Force

Figure B-1l: CB Sliding Evaluation - Concrete Fill Bottom Reactions Time Histories from UB Full Column Profile Analysis Case 12

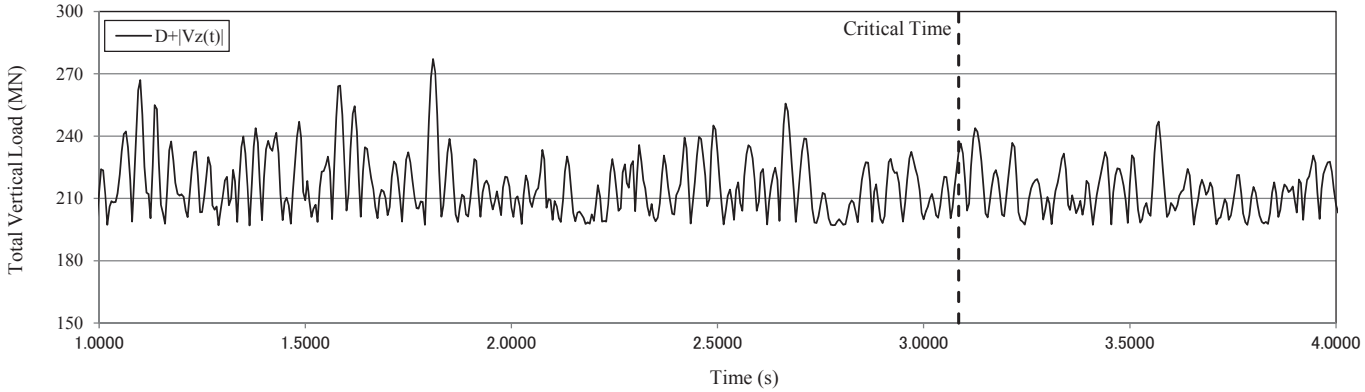

(a) Total Vertical Load with Upward Seismic Reaction

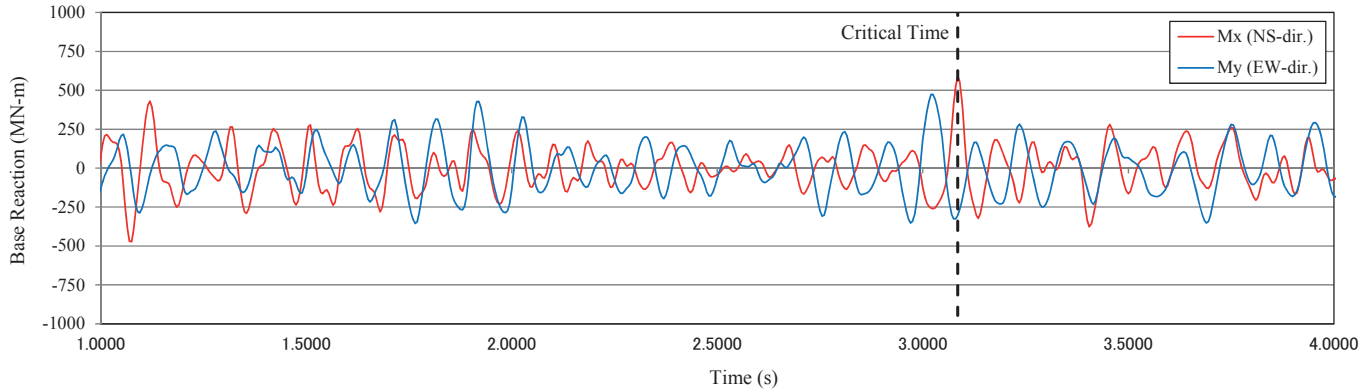

(b) Overturning Moments

Figure B-2a: CB Bearing Pressure Calculations – Basemat Bottom Reactions Time Histories from LB Partial Column Profile Analysis Case 7

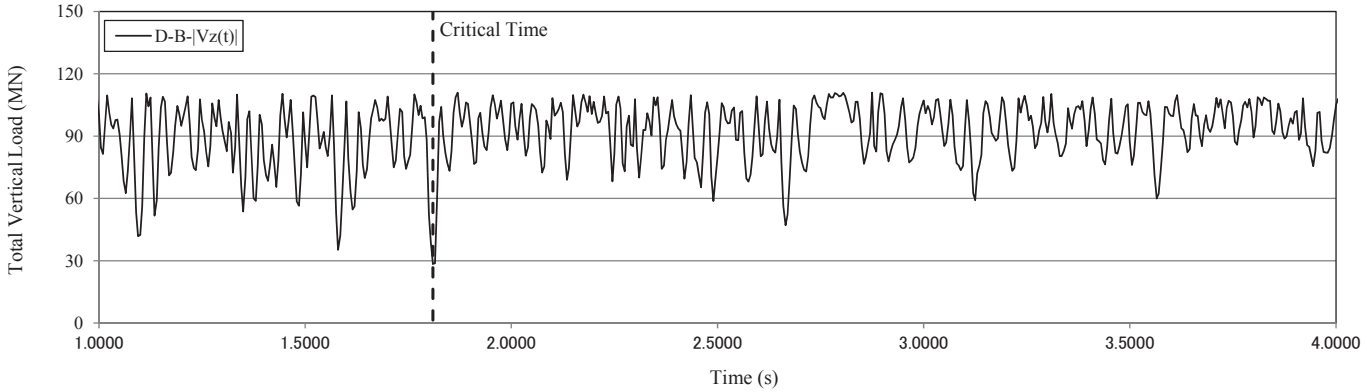

(a) Total Vertical Load with Upward Seismic Reaction

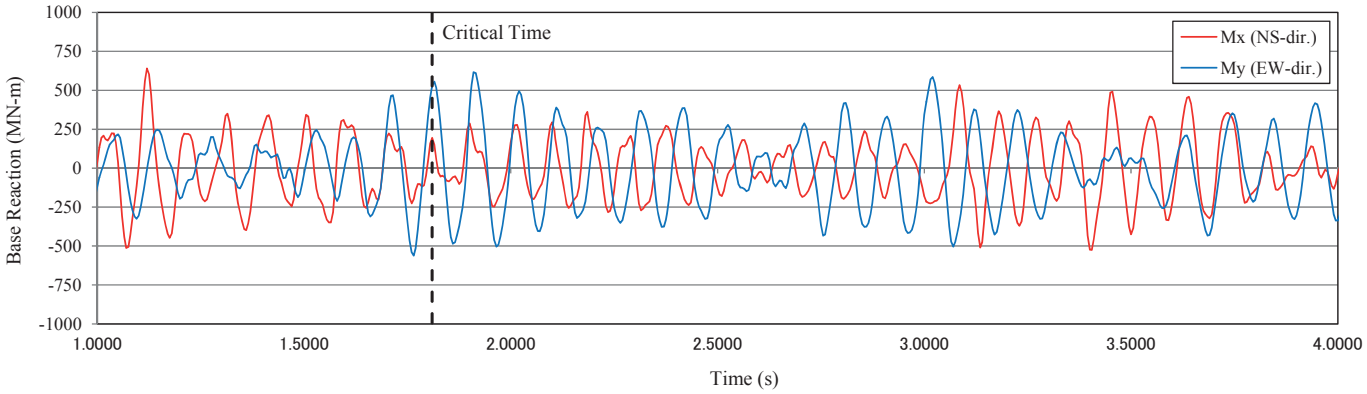

(b) Overturning Moments

Figure B-2b: CB Bearing Pressure Calculations – Basemat Bottom Reactions Time Histories from BE Partial Column Profile Analysis Case 8

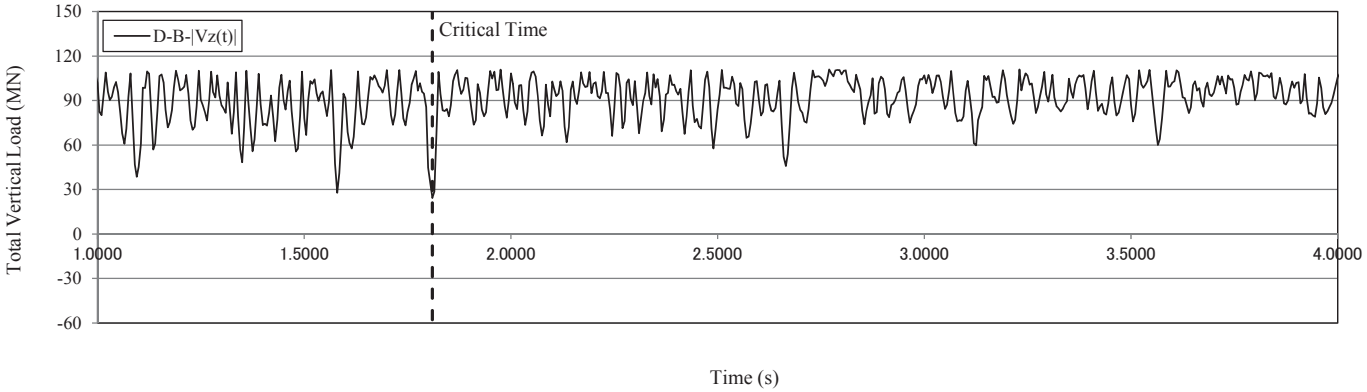

(a) Total Vertical Load with Upward Seismic Reaction

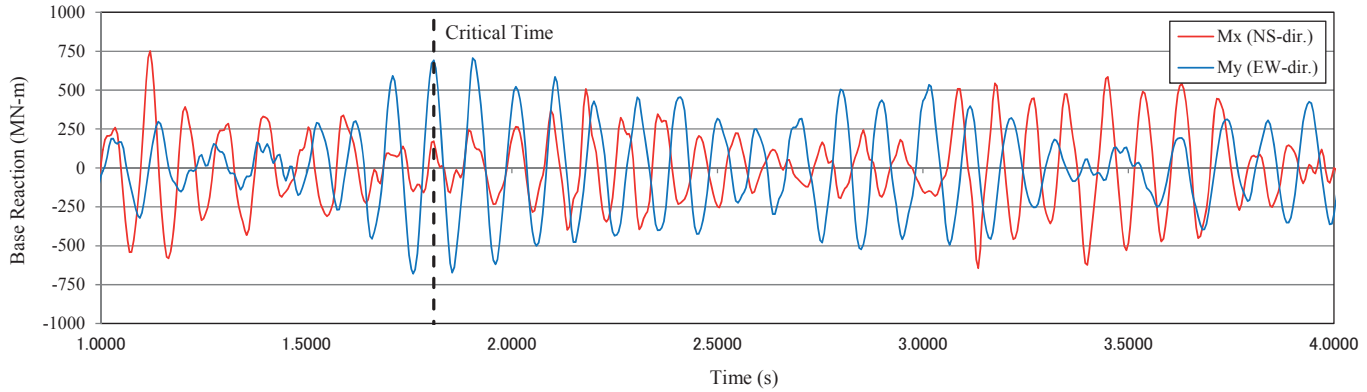

(b) Overturning Moments

Figure B-2c: CB Bearing Pressure Calculations – Basemat Bottom Reactions Time Histories from UB Partial Column Profile Analysis Case 9

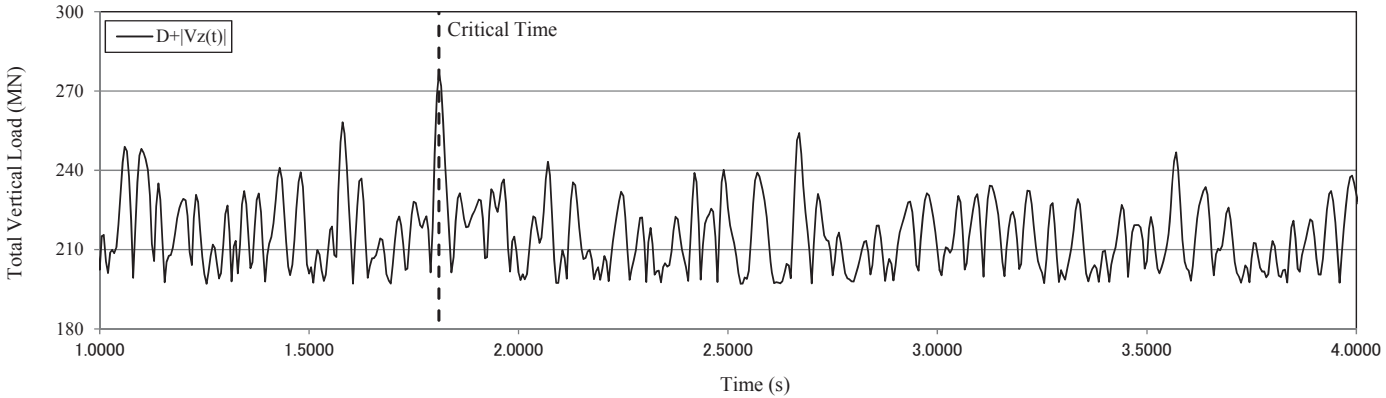

(a) Total Vertical Load with Downward Seismic Reaction

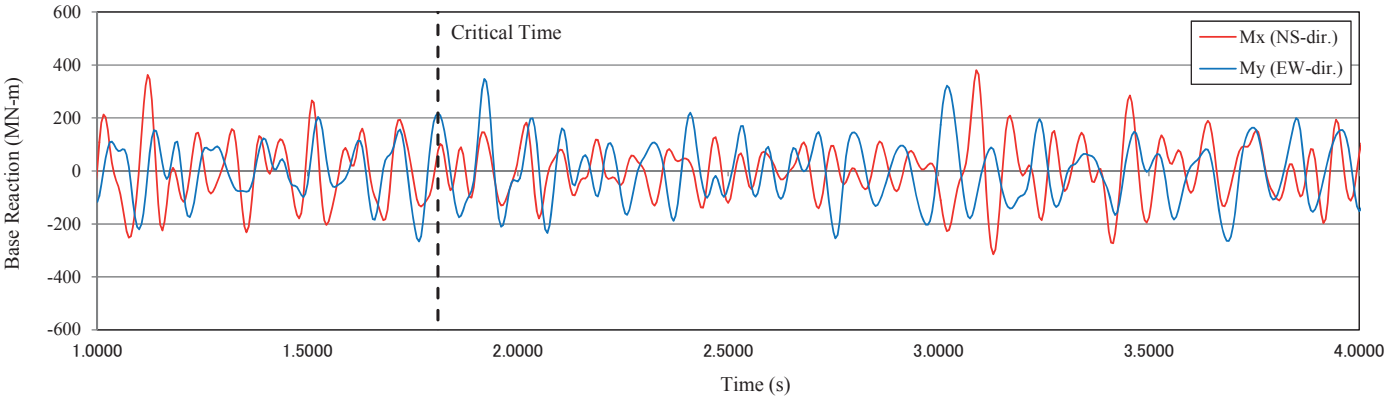

(b) Overturning Moments

Figure B-2d: CB Bearing Pressure Calculations – Basemat Bottom Reactions Time Histories from LB Full Column Profile Analysis Case 10

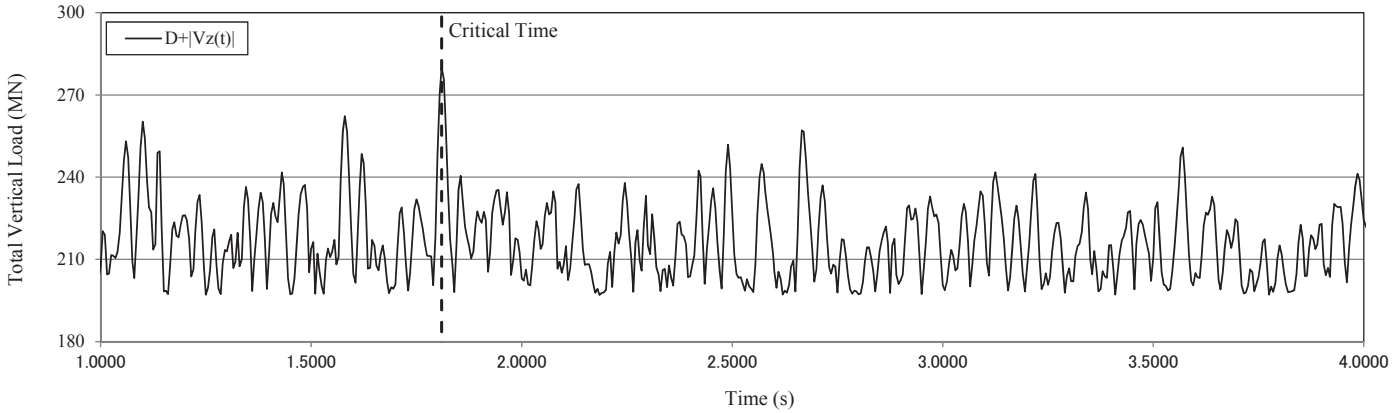

(a) Total Vertical Load with Downward Seismic Reaction

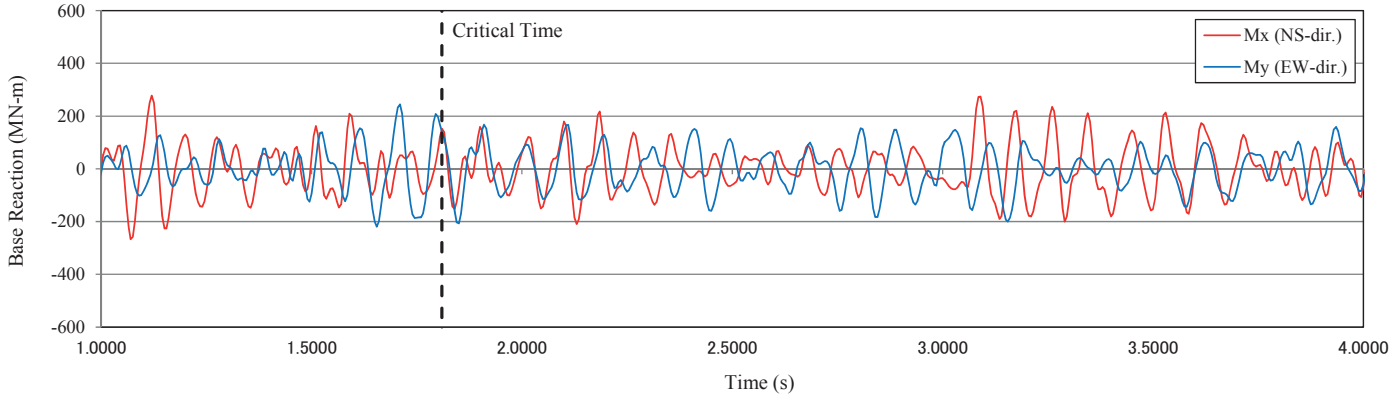

(b) Overturning Moments

Figure B-2e: CB Bearing Pressure Calculations – Basemat Bottom Reactions Time Histories from BE Full Column Profile Analysis Case 11

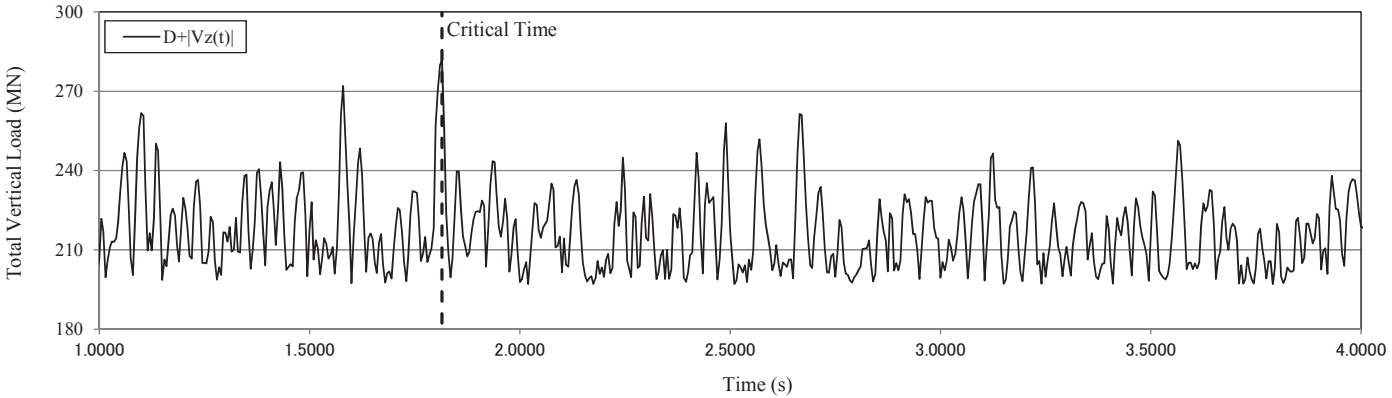

(a) Total Vertical Load with Downward Seismic Reaction

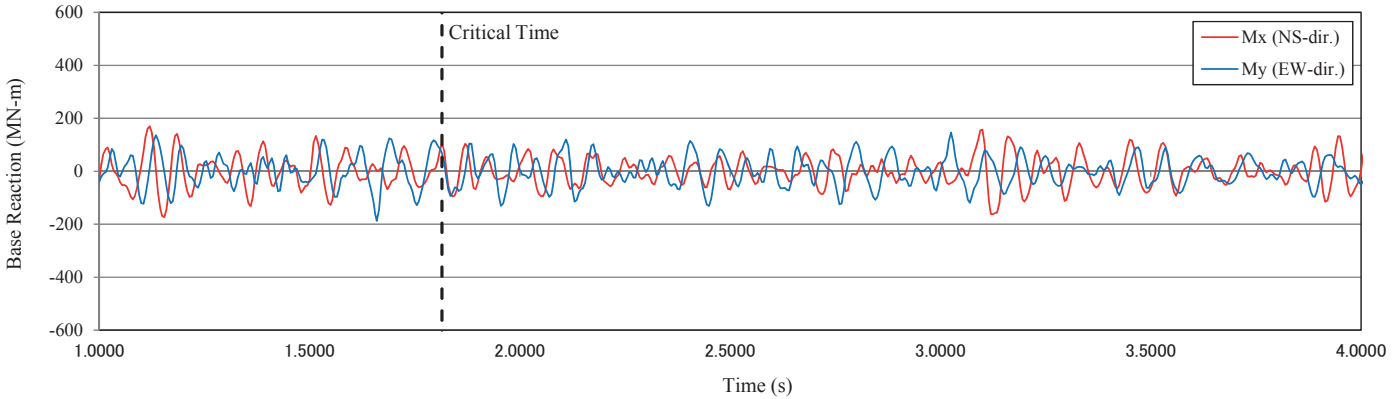

(b) Overturning Moments

Figure B-2f: CB Bearing Pressure Calculations – Basemat Bottom Reactions Time Histories from UB Full Column Profile Analysis Case 12

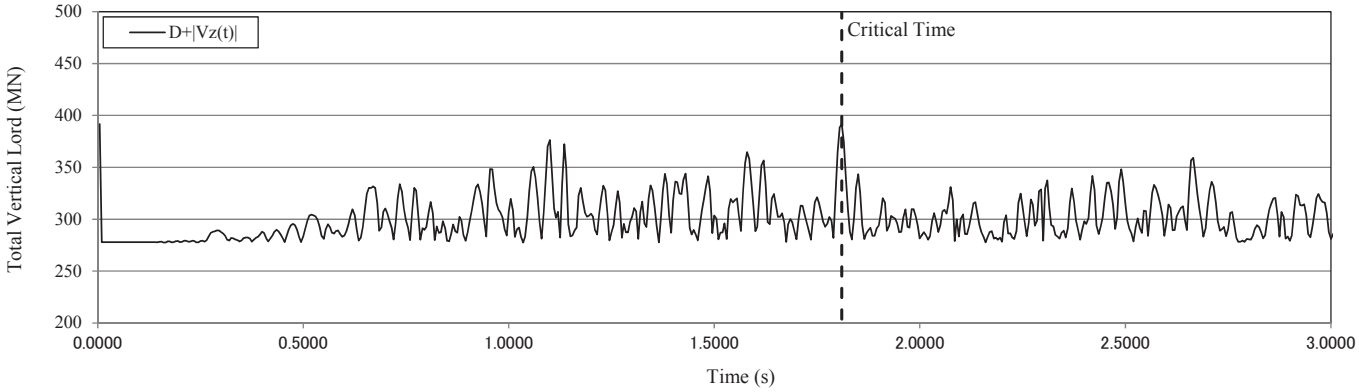

(a) Total Vertical Load with Downward Seismic Reaction

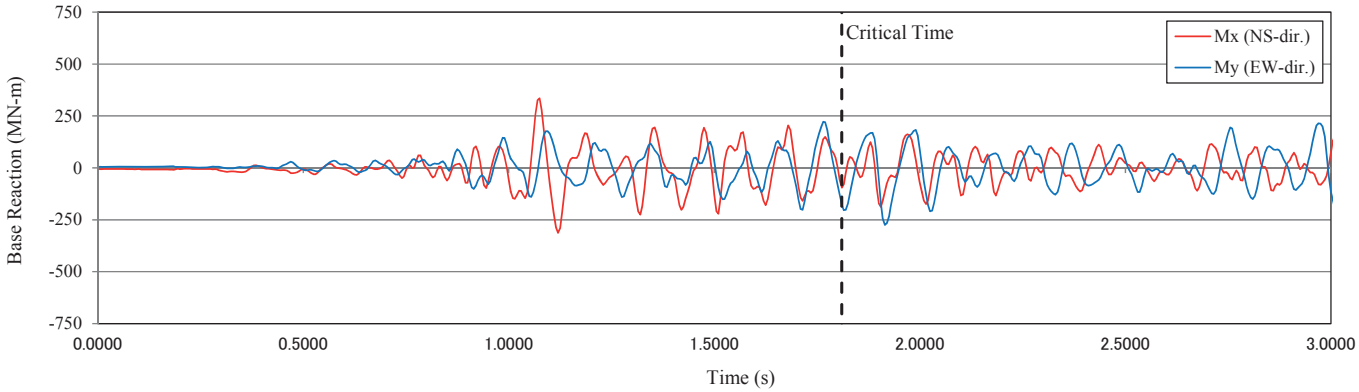

(b) Horizontal Driving Seismic Force

Figure B-2g: CB Bearing Pressure Calculations – Concrete Fill Bottom Reactions Time Histories from LB Partial Column Profile Analysis Case 7

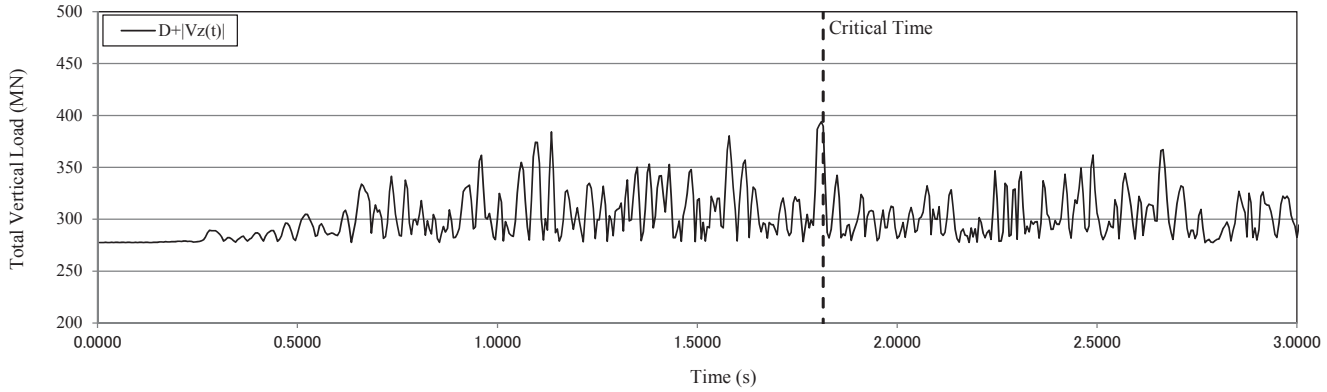

(a) Total Vertical Load with Downward Seismic Reaction

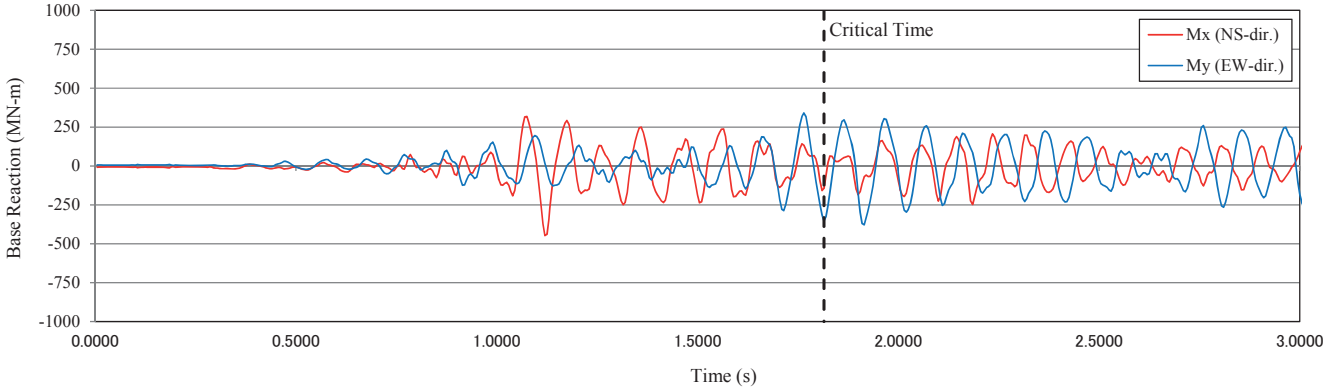

(b) Horizontal Driving Seismic Force

Figure B-2h: CB Bearing Pressure Calculations - Concrete Fill Bottom Reactions Time Histories from BE Partial Column Profile Analysis Case 8

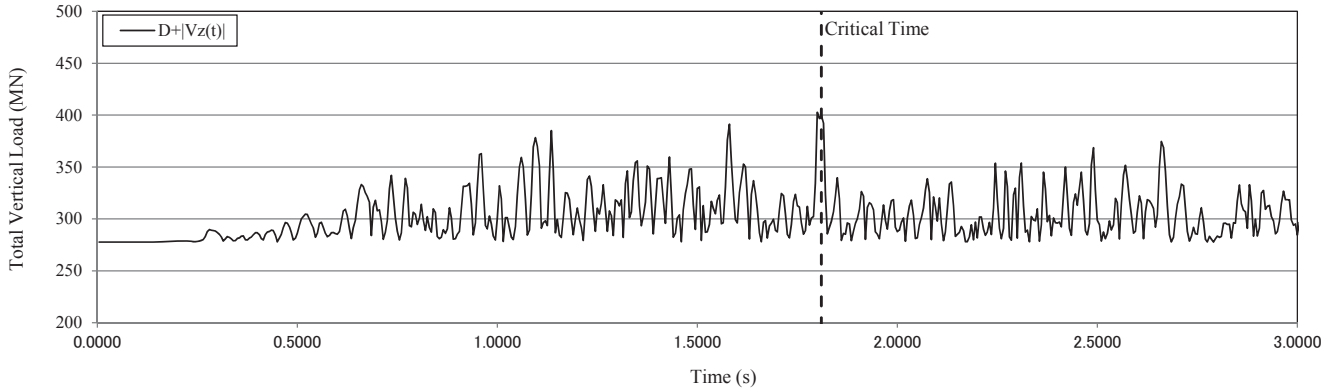

(a) Total Vertical Load with Downward Seismic Reaction

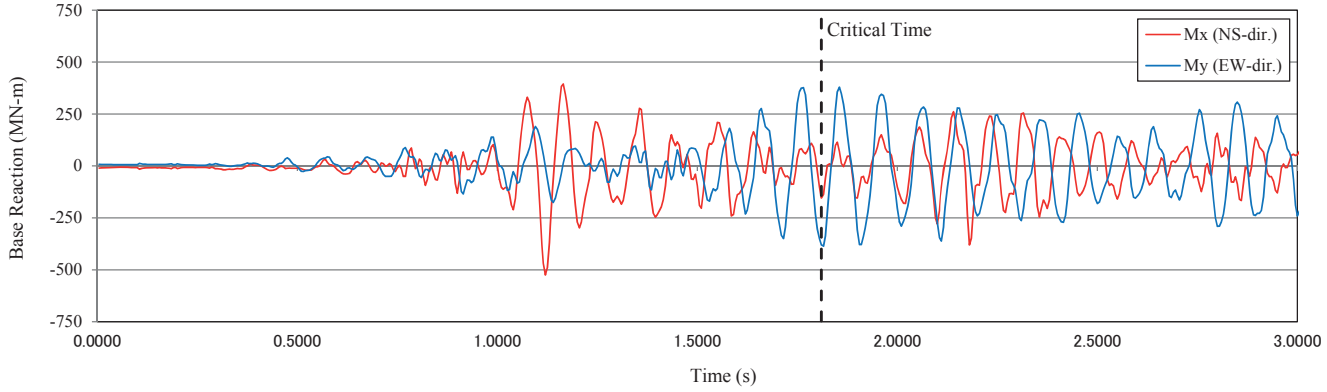

(b) Horizontal Driving Seismic Force

Figure B-2i: CB Bearing Pressure Calculations - Concrete Fill Bottom Reactions Time Histories from UB Partial Column Profile Analysis Case 9

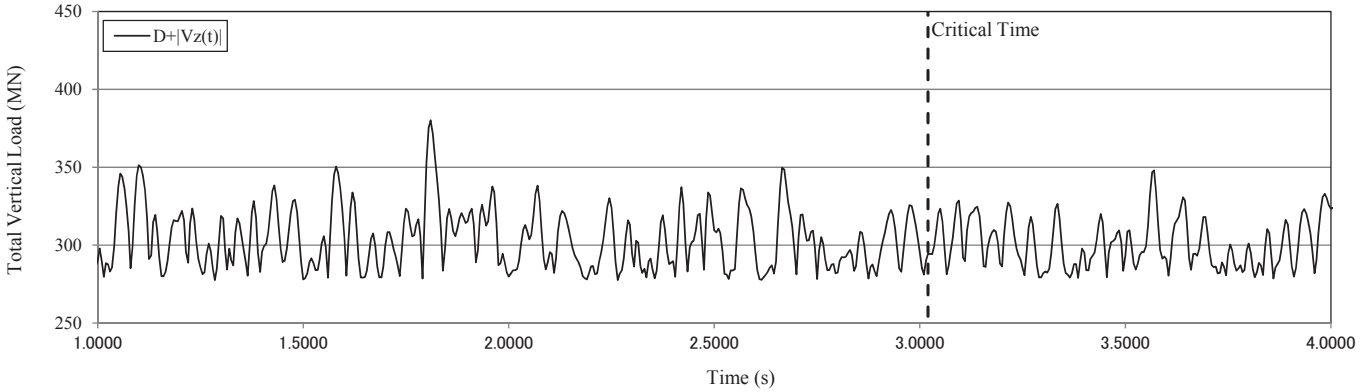

(a) Total Vertical Load with Downward Seismic Reaction

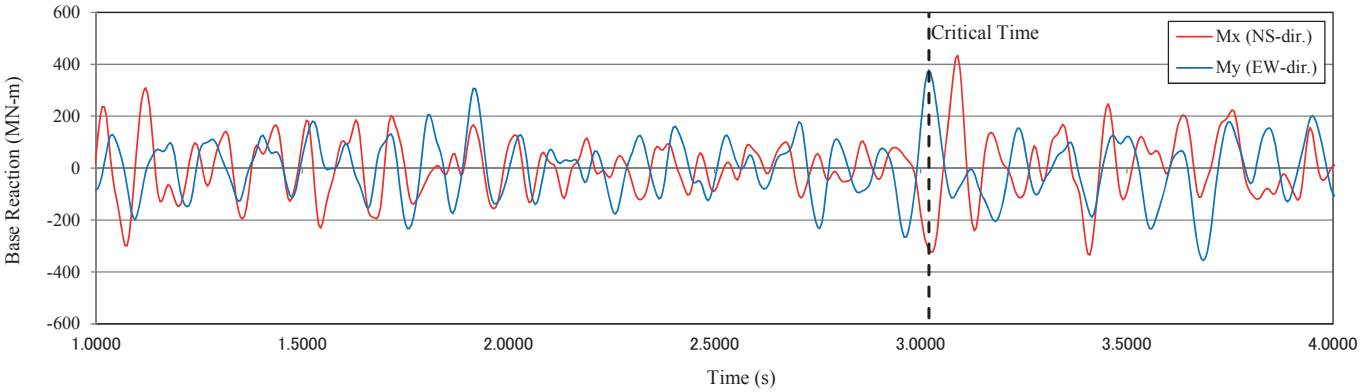

(b) Horizontal Driving Seismic Force

Figure B-2j: CB Bearing Pressure Calculations - Concrete Fill Bottom Reactions Time Histories from LB Full Column Profile Analysis Case 10

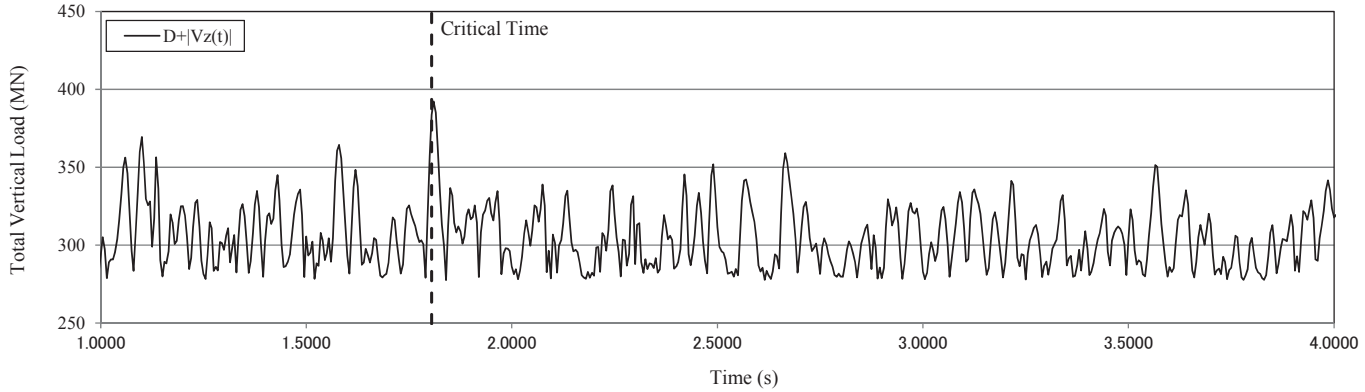

(a) Total Vertical Load with Downward Seismic Reaction

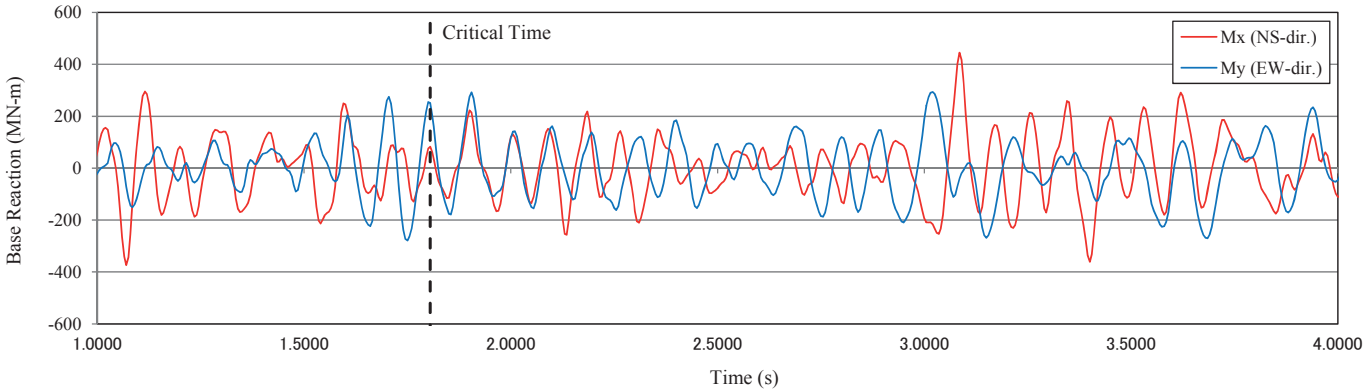

(b) Horizontal Driving Seismic Force

Figure B-2k: CB Bearing Pressure Calculations - Concrete Fill Bottom Reactions Time Histories from BE Full Column Profile Analysis Case 11

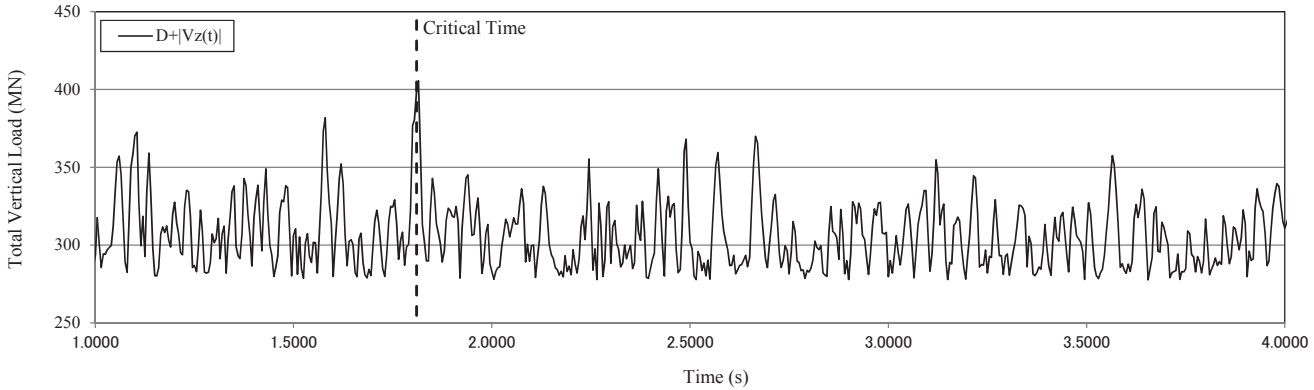

(a) Total Vertical Load with Downward Seismic Reaction

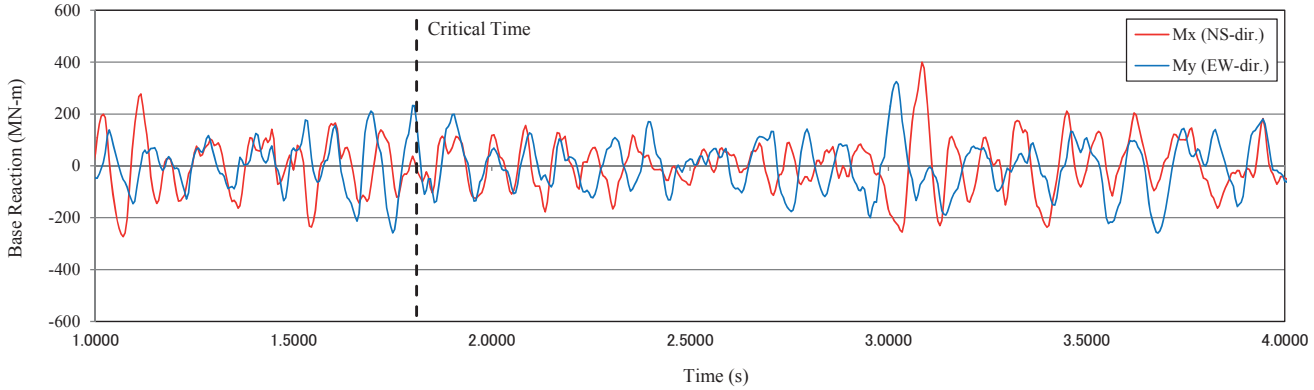

(b) Horizontal Driving Seismic Force

Figure B-2l: CB Bearing Pressure Calculations - Concrete Fill Bottom Reactions Time Histories from UB Full Column Profile Analysis Case 12